QATAR UNIVERSITY

COLLEGE OF ENGINEERING

FABRICATION OF FOULING RESISTANT TI3C2TX (MXENE)/CELLULOSE ACETATE NANOCOMPOSITE MEMBRANE FOR FORWARD OSMOSIS APPLICATION

BY

RADWAN AHMAD FIRAS ALFAHEL

A Thesis Submitted to

the College of Engineering

in Partial Fulfillment of the Requirements for the Degree of

Masters of Science in Civil Engineering

June 2020

COMMITTEE PAGE

The members of the Committee approve the Thesis of
Radwan Ahmad Firas Alfahel defended on 15/04/2020.

Dr. Alaa H. Hawari
Thesis/Dissertation Supervisor

Approved:

Khalid Kamal Naji, Dean, College of Engineering

ABSTRACT

ALFAHEL, RADWAN, A. F. , Masters : June : 2020, Masters of Science in Civil Engineering

Title: Fabrication of Fouling Resistant Ti3C2Tx (MXene)/Cellulose Acetate Nanocomposite Membrane for Forward Osmosis Application

Supervisor of Thesis: Alaa, H, Hawari.

Forward Osmosis (FO) is one of the promising technologies that can be used to combat growing water scarcity. However, FO membrane fouling hinders the widespread application of this technology by significantly reducing the water flux and membrane lifecycle. Although forward osmosis has shown lower membrane fouling when compared to other membrane technologies, forward osmosis membrane resistance to fouling must still be improved. In this study, $Ti_3C_2T_x$ (MXene) was used to improve the fouling resistance of FO flat-thin film membranes. The mixed-matrix $Ti_3C_2T_x$ (MXene)/ cellulose acetate (CA) membranes with different (wt%) loading of MXene were fabricated by covalent crosslinking followed by phase inversion method. The fabricated membranes were characterized by X-ray powder diffraction (XRD), energy-dispersive X-ray spectroscopy (EDS), contact angle measurement and scanning electron microscopy (SEM). The performance of the fabricated FO membranes was evaluated utilizing seawater as draw solution (DS) and two feed solutions (FS) namely; distilled water (DI) and treated sewage effluent (TSE). The water flux, reverse solute flux and the rejection of dissolved solids were evaluated in the FO process. It was observed that the cross-linked cellulose acetate membrane with 8 wt% MXene (CCAM-8%) showed higher resistance to fouling when compared with commercial thin-film

composite (TFC) FO membrane, the water flux of CCAM-8% decreased by only 10.7% using TSE as FS compared to DI, where the water flux of the TFC commercial membrane decreased by 32.2% when using TSE as FS compared to DI.

DEDICATION

This work is dedicated to my parents. Also, to my friends who supported me.

ACKNOWLEDGMENTS

I would like to thank Dr. Alaa Al-Hawari my supervisor for his massive support. Also, I would also like to thank Dr. Mohamed Hassan for his guidance through the project.

TABLE OF CONTENTS

LIST OF TABLES

LIST OF FIGURES

LIST OF ABBREVIATIONS

AL	Active Layer
AL-DS	Active Layer Facing Draw Solution
AL-FS	Active Layer Facing Feed Solution
BOD	Biological Oxygen Demand
CA	Cellulose Acetate
CCAM	Cross-linked Cellulose Acetate Membrane
CECP	Concentrative External Concentration Polarization
CICP	Concentrative Internal Concentration Polarization
CP	Concentration Polarization
CTA	Cellulose Triacetate
DECP	Dilutive External Concentration Polarization
DI	Distilled Water
DICP	Dilutive Internal Concentration Polarization
DL	Delaminated
DS	Draw Solution

ECP	External Concentration Polarization
FO	Forward Osmosis
FS	Feed Solution
ICP	Internal Concentration Polarization
MEF	Multi Effect Flash
ML	Multi-layered
MSF	Multi Stage Flash
PA	Polyamide
PRO	Pressure Retarded Osmosis
POM-OFs	Polyoxometalate based open frameworks
RO	Reverse Osmosis
RSF	Reverse Solute Flux
SEM	Scanning Electron Microscopy
SL	Support Layer
SW	Seawater
TDS	Total Dissolved Solids

TFC	Thin Film Composite
TFN	Thin Film Nanocomposite
TS	Total Solids
TSE	Treated Sewage Effluent

CHAPTER 1: INTRODUCTION

1.1 Overview

Forward Osmosis (FO) is a process that uses the osmotic pressure gradient between a feed solution (FS) and a draw solution (DS) as the driving force instead of the hydraulic pressure (Altaee, Mabrouk, & Bourouni, 2013; S Thabit et al., 2019). Therefore, the operating cost of FO is lower than any other membrane-based separation process. The forward osmosis process has paid significant attention in the last decade especially when compared to other membrane separation technologies (i.e. reverse osmosis (RO), nanofiltration (NF), and microfiltration (MF)). This is due to the low energy consumption, high water recovery and low membrane fouling (Ang, Wahab Mohammad, Johnson, & Hilal, 2019; Shaffer, Werber, Jaramillo, Lin, & Elimelech, 2015). Although forward osmosis has shown lower membrane fouling when compared to other membrane technologies, forward osmosis membrane resistance to fouling must still be improved. Extensive development of FO membranes have been created during the last decade. Multiple Thin Film Composite (TFC), Phase inversion, Layer by layer (LbL) and cellulose acetate (CA) membranes have been developed (Chou et al., 2010; Ong, Chung, Helmer, & de Wit, 2012; L. Shi et al., 2011; K. Y. Wang, Chung, & Amy, 2012; K. Y. Wang, Yang, Chung, & Rajagopalan, 2009).

In general, a high-performance FO membrane must have the following characteristics: high anti-fouling properties, a thin active layer of high salt rejection and water permeability, and a support layer that is highly porous for the reduction of internal concentration polarization.

1.2 Objectives

In this study, a new membrane was fabricated by covalent interaction of $Ti_3C_2T_x$ (MXene) with CA followed by phase inversion processing to develop an FO membrane for wastewater reclamation and water desalination. The addition of MXene into the CA

polymeric matrix is expected to enhance fouling resistance and water flux of the membrane. The performance of the synthesized membrane was evaluated in a FO process in terms of water flux and reverse solute flux.

1.3 Thesis layout

Water challenges in Qatar and challenges to treat wastewater were demonstrated in the first part of this thesis. Then, a literature review is prepared in addition to a summary for the most recent research done in fabrication of FO membranes. Later, methods and materials used in FO process and MXene/CA membrane were described. Characterization and testing procedures were described. Also, the results of FO presented, described and discussed. Lastly, conclusions of the work done were stated.

CHAPTER 2: LITERATURE REVIEW

2.1 Water statistics in Qatar

With a growing economy, the demand for freshwater in Qatar is increasing every day. Qatar is the second in water consumption per capita in the world. The water consumption was 0.7 m^3/day/person in 2015. Also, the total consumption for industrial and residential usage was 706.1 Million m^3 of freshwater *(WATER STATISTICS In The State of Qatar, 2015, 2017)*. The demand for water in State of Qatar comes from industrial, residential, and agricultural sectors. Nowadays, the water demand is met ~68% by desalination plants, ~30% by underground water, and approximately 2% by treated sewage effluent (TSE). The increasing trend of water consumption in State of Qatar is shown in Figure 1. It can be seen that since 2005, the consumption level of groundwater has not changed. Therefore, extracting more groundwater to meet the increasing demand is not an efficient solution.

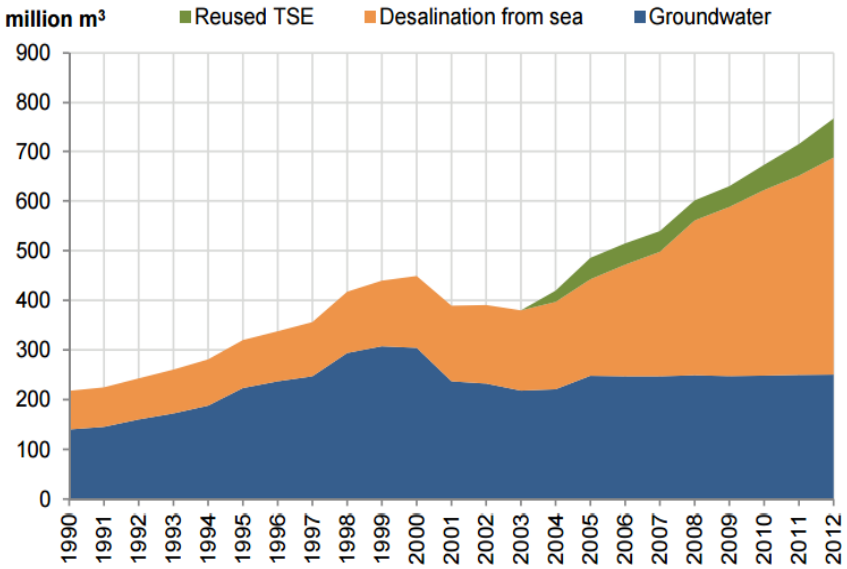

Figure 1. Source of freshwater in Qatar (WATER STATISTICS In The State of Qatar, 2015, 2017).

2.1.1 Ground water

The agricultural sector in Qatar is the main user of the groundwater from aquifers. In 2013, 250 Million m3 of the groundwater in Qatar were extracted (WATER STATISTICS In The State of Qatar, 2015, 2017). Though, the aquifers total recharge from inflow and rainfall from Saudi Arabia was only 48 Million m3. This disparity possesses are a significant threat to freshwater aquifers. The flow of seawater to groundwater is a direct consequence of this disparity and the water salinity is on rise as indicated by the conductivity of underground water samples. Currently, there are three main with saline water, desalinated has been injected to the ground.

2.1.2 Desalination plant

Desalinated water is utilized for residential and industrial purposes. The most recent available data has been published in 2018 shows that, total desalination capacity in state of Qatar is1.69 Million m^3/day (MIGD) or 480 Million Imperial Gallons per

Day ("Overview on- KAHRAMAA drinking water quality requirement.," 2014).

Currently, there are three main desalination technologies used globally: Multi Effect Flash (MEF), Multi Stage Flash (MSF), and RO (Burn et al., 2015). In multi stage flash technology, the brine is heated to 95-110^{o}C (Hanshik, Jeong, Jeong, & Choi, 2016). The brine was evaporated partly by the flash columns. There are 17 to 40 flash columns. The incoming brine is heated up by the vapor coming from each flashing unit (Harandi, Rahnama, Jahanshahi Javaran, & Asadi, 2017). The first 20-30 stages where brine is heated utilizing the vapor comes from flashing, is known as heat recovery stages. Heat rejection stages are the last 3-10 stages (Fiorini & Sciubba, 2005). Figure 2 shows a schematic diagram of an MSF desalination plant.

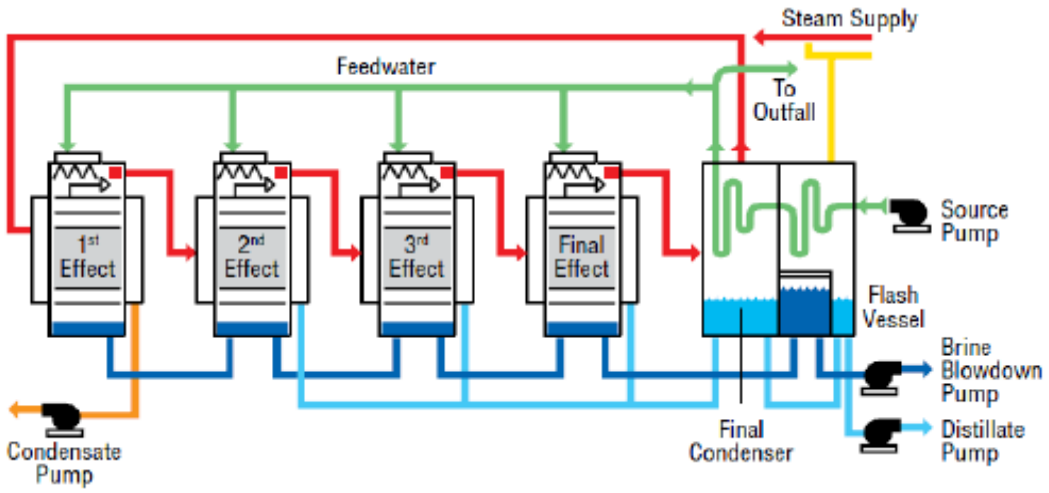

Figure 2. Schematic of a MSF desalination plant (Lingkungan, 2012)

In multi effect flash distillation, steam is supplied to the first flashing column (Ullah, Rasul, & Khan, 2013). The brine inside the column gets heated by steam and

evaporates. The vapour from first flashing stage enters the second flashing stage and evaporates the brine in second flashing stage. The vapour continues to follow this pattern until the last flashing stage. The vapour from all the stages are finally condensed and collected as fresh water (El-Dessouky, Ettouney, Al-Juwayhel, & Al-Fulaij, 2004). It is to be noted that, the pressure inside the column decreases gradually in the flash drums. This in turn reduces the boiling point of brine inside the flash column (Bromley & Read, 1970). The number of flash columns can be between 20 and 25. Figure 3 shows a schematic diagram of a MEF desalination process with 3 flash columns.

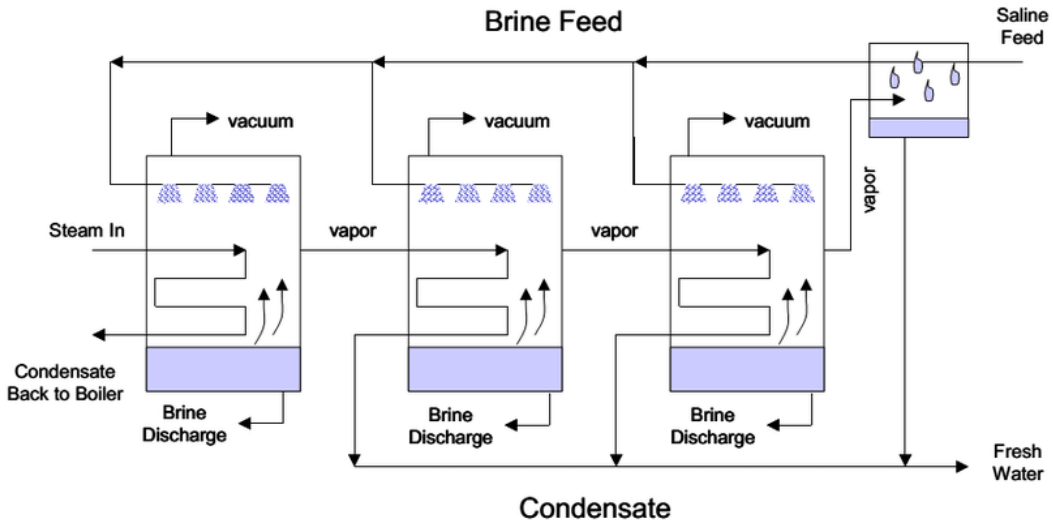

Figure 3. Schematic diagram of a MEF desalination process (Ullah et al., 2013).

Another technology that is widely used for small scale desalination plants is Reverse Osmosis. In reverse osmosis, there are two sides of the filters. Due to osmotic pressure, the natural direction of water is from the higher concentration side to the lower concentration side (Malaeb & Ayoub, 2011). In RO, the hydrostatic pressure of the brine is increased above the solution osmotic pressure. This positive-pressure gradient

generates concentration gradient across the membrane against the natural-osmosis direction (Greenlee, Lawler, Freeman, Marrot, & Moulin, 2009).

Almost 98% of the desalinated water comes from MSF and MEF desalination plants ("Overview on- KAHRAMAA drinking water quality requirement.," 2014).

As seen from **Error! Not a valid bookmark self-reference.**, the main desalination technologies suitable for Qatar are expensive thermal desalination plants. In order to decrease the stress of desalination and ground water, usage of TSE has to be increased.

Table 1. Desalination Plants in Qatar (2018)

Name	Capacity (MIGD)	Technology
Raas Abo Funtas B	33.0	MSF
Raas Abo Funtas B3	29.2	MSF
Raas Abo Funtas A1	45.0	MSF
Raas Abo Funtas A2	36.0	MSF
Raas Abo Funtas A3	36.0	MSF
Dukhan	2.0	RO
Ras Laffan Power	40.0	MED
Qatar Power	60.0	MED
Ras Girtas Power	63.0	MED
Umm Al Houl Power	136.0	RO/MSF
Total	480.2[1]	

1) 2.2 Million m3/day

2.2 Treated sewage effluent

The sewage effluent in state of Qatar is treated and be utilized mainly for landscaping and agriculture. In 2011, 15.7% of the total water demand of agriculture industry was met by Treated Sewage Effluent (TSE). In 2012, the percentage increased to 28.0%. Rather than agriculture, TSE is being utilized by the industries of district

cooling (ASHGAL, 2014). It is illegal in state of Qatar to utilize tap water for cooling. It is estimated that by the year 2020, 73 Million m^3 of TSE will be utilized by cooling industries (Jasim, Saththasivam, Loganathan, Ogunbiyi, & Sarp, 2016). Also, there are other sector that are using TSE in state of Qatar such as fire-fighting training exercises, sand washing, sanitary flushing and non-potable utilize in road works and construction. Qatar aims to extend their facilities of sewage treatment to meet the demand of about 1.1 Million people by 2020 ("Qatar progresses with wastewater reuse plan," 2016). Table 2 shows the wastewater treatment plants in state of Qatar.

As seen from Table 2, there are several stages utilized by all the WWTPs to make TSE appropriate for discharging. The stages could be divided into primary, secondary and tertiary treatment stages.

Table 2. Wastewater Treatment Plant in Qatar (2019)

Plant	Capacity (m^3/d)	Main stages	Tertiary treatment
Doha north sewage treatment works	439,000	Fine Screen – Grit Separator – Bioreactor – Clarifier – Chlorine contact tank – GMF – Ultrafiltration – UV disinfection.	Ultrafiltration + UV disinfection
Doha south sewage treatment works	241,000	Screening - Grit removal - Aeration tanks - Clarifiers - Sand filter- Chlorination	Ultrafiltration
Doha west sewage treatment works	175,500	Screening (6 mm) - Grit traps (VORTEX type) - Aeration tanks – Blowers - Clarifiers (suction type) - Sand filters - Membranes filtration.	Ultrafiltration (Ultrablue™ ZW1000)
Lusail sewage treatment works	60,000	screening (10 mm) – equalization - fine screening - grease removal and cooling - membrane bioreactor – Ultrafiltration – Chlorination.	UltraforTM MBR membrane bioreactor + Ultrafiltration + Chlorination

2.2.1 Preliminary and primary treatment

Wastewater preliminary and primary treatment usually contains combination of technologies designed to remove coarse biodegradable material and grit from wastewater and stabilize the stream by chemical additions. In domestic water treatment, preliminary and primary processes can remove up to 25% of the organic matter and approximately the entire nonorganic matter (Salgot & Folch, 2018). In industrial wastewater treatment, primary treatment processes may include pH adjustment and equalization of flow that is extremely important to the treatment plant (Ardley, Arnold, Younker, & Rand, 2019).

A crucial part of the wastewater recycling plant is the facilities and equipment used to eliminate grit, rags, sticks, debris and other undesirable objects (Salgot & Folch, 2018). This may cause severe damage to the facility and reduce the treatment efficiency. A summary of the commonly used unit operations is listed below.

(1) Screening. Screening is a preliminary treatment process used to intercept unwanted solids, to protect mechanical equipment in the treatment plant and prepare the main wastewater stream to enter through the process. Screening shall always be used for different types of wastewater.

(2) Grit removal. Grit is defined as heavyweight inactive particles in the wastewater stream which will not be able to decompose. Grit has a S.G of 2.65, and design of grit removal chambers is done to remove the particles larger than about 0.011 inch (Hernández-Chover, Bellver-Domingo, & Hernández-Sancho, 2018).

(3) Pre-aeration. This is done by pumping oxygen to the wastewater stream in stage of preliminary treatment. This is conducted by either increasing the detention

time in the aerated chamber or separate additional aeration process (Y. Liu et al., 2019).

(4) Equalization. Equalization is usually used for industrial discharges wastewater and some military processes. Equalization process decreases fluctuations of the influent to levels which make it suitable for succeeding processes. A proper facility regulates the wide variations of flow, pH, biological oxygen demand (BOD), and other parameters to make it suitable for downstream systems. Appropriate equalization stage will minimize system problems and provide a higher-quality effluent.

(5) pH control. pH control is used in preliminary treatment of industrial wastewater treatment. Treatment plant equipment can be damaged because of acidic or basic steam (Hernández-Chover et al., 2018). This process is important to meet effluent quality necessary for secondary stage.

(6) Flotation is usually used to treat wastewater with high amount of grease and fine suspended particles. This is found in discharges and streams created by industrial application. Domestic wastewater may also contain grease because of food deposits (Ardley et al., 2019). Using aeration to float materials may release scum in a sedimentation tank and reduce the grease concentration to make it suitable for the following treatment processes. Grit removal is usually combined with the flotation process by introducing sludge-removal facility (Hernández-Chover et al., 2018).

(7) Plain sedimentation. gravity sedimentation is usually done after the preliminary treatment in an inactive tank. In this process, most of the settable solids and suspended solids settle in the basin. Mechanical collectors are used to remove the sludge from the wastewater surface. Skimming is also provided to eliminate

floatable particles such as oil, grease and scum that gather at the surface (Brusseau, Famisan, & Artiola, 2004). Wastewater characteristics and the amount of organics present in the solids plays major role in determining the BOD and suspended solids removal efficiency.

(8) Chemical coagulation. Sedimentation using chemical coagulation is applied to remove the phosphate from the domestic wastewater and other elements in industrial wastewater. The removal of BOD and suspended solids is enhanced by chemical coagulating, but it is not usually economical. However, it is used in some specific applications (Hernández-Chover et al., 2018).

2.2.2 Secondary treatment

Secondary wastewater treatment usually contains processes such as coagulation-flocculation, oxidation, precipitation by using biological processes where bacteria are used to remove the pollutant. Biological treatment is used to remove the organic-matter from the wastewater. Hence, biological reactor is usually used in secondary treatment process either in single stage or in multi stage as per the requirements to comply with the discharge standards (J. Tang, Zhang, Shi, Sun, & Cunningham, 2019).

Wastewater biological treatment is done to remove organic substance from the stream which is available in colloidal and soluble form. In addition, it aims to reduce the concentration of nutrients such as phosphorous and nitrogen from wastewater. Cell tissue has high density compared to water, so it can be removed in settling tank. Hence, the cell tissues need to be removed before the process ends.

Biodegradable organics are biologically removed by multiple steps including absorption, adsorption, mass transfer, and biochemical enzymatic reactions. Treatment of organic substances is accomplished by two distinct metabolic processes:

(1) Respiration. organic and inorganic particles are oxidized by the biochemical reactions, which is catalyzed by large protein molecules (enzymes) produced by microorganism. The oxidation process takes place in both anaerobic and aerobic conditions. In aerobic conditions, the final electron is accepted by oxygen. In anaerobic conditions, the final electron is accepted by nitrates, sulphates, carbon dioxide and other organic compounds (Z.-H. Li, Hang, Lu, Zhang, & Yu, 2019). Respiration metabolic products are true inorganics such as carbon dioxide, hydrogen sulfide, water and ammonia. The energy obtained from the respiration is consumed by the microorganisms to create new protoplasm through another group of reactions. The heterotrophic microorganisms originate the energy needed for cell synthesis by oxidation of organic matter (Hernández-Chover et al., 2018). Autotrophic microorganisms derive the energy for synthesis either from the photosynthesis or the inorganic substances. Microorganisms require energy for the maintenance of their life activities.

(2) Catabolism and Anabolism. bacterial metabolism is one of the most important process to remove the organic material from the wastewater. Metabolism is the usage of the organic material as a source of energy for the production of cellular matter. Catabolism is the process of transferring the organic material into stable end product while using it as source of energy. Anabolism is the process of incorporating the organic material into cell mass. Anabolism process consumes energy and it is only possible if catabolism occurs at parallel time to supply the required energy.

2.2.3 Tertiary treatment

It is the last treatment process that polish the wastewater to make it suitable to being reused, recycled or discharged. This stage treatment eliminates the traces of the

nitrogen and phosphorus. Bacteria and viruses are also removed at this stage because it is harmful for the human body.

(1) Physical processes of tertiary treatment. The physical method used for tertiary wastewater treatment depends on passing of the stream through sand-filters or micro screen. The wastewater passes through micro pores which attract fine suspended particles. The particles retention is specified by the pores size. The water enters through the frontal side of the sieve, where suspended solids rest on the sieve surface and water passes to the other side of the sieve. In addition, sand filters can be used in tertiary wastewater treatment which is similar to the sieve. Sand filter is more efficient than micro screens, however it decreases the amount of dissolved oxygen in the wastewater sample (Sharma, Syed, Brighu, Gupta, & Ram, 2019). Micro screen is easier to operate compared to sand filter. Treatment using UV is usually done to prevent the bacterial growth in the treated sample.

(2) Physicochemical processes of tertiary treatment. In tertiary treatment stage more physicochemical methods can be applied such as: chemical coagulation, adsorption, electrodialysis, foaming, distillation, reverse osmosis, solvent extraction, freezing, ionic exchange, chemical and electrochemical oxidation.

The water coming out from the tertiary treatment stage is usually discharged back to the water bodies. However, these treated sewage effluents (TSE) have the potential to be engineered to fertilizing solution after further treatment.

2.3 Forward osmosis

Osmosis is the process that explains the solvent diffusion through a semi-

permeable membrane and the rejection of solute particles. This process was primarily considered by Wilhelm Pfeffer in 1877. Later on, it was presented again by Thomas Graham. When two different solutions with low and high concentrations are detached by a semi-permeable membrane, the pure water particles moved from low to high concentration until they reach equilibrium. Osmotic pressure is a natural chemical process generated by the chemical solution and can be calculated utilizing equation (1) which is applicable for ideal solutions.

$$\pi = nMRT \qquad (1)$$

Which n is Van't Hoff factor, R is ideal gas constant (R=8.3145 $J \cdot K^{-1} \cdot mol^{-1}$), M is molarity and T is the temperature (°C).

FO membranes contain two different layers one called active layer (AL) and the other called support layer (SL). The dense AL is casted to a porous SL which allows the forward osmosis membranes to have the nature of asymmetry (Zhao, Zou, Tang, & Mulcahy, 2012). As a result, the are two operation modes for FO process, FO and pressure retarded osmosis (PRO). In PRO mode, the AL is facing the DS while in FO mode, the AL is facing FS.

FO came as a promising desalination technology and it is counted as a clean process in terms of energy. FO is a process that doesn't need external pressure to be applied, so, it depends on the difference of osmotic pressure between DS and FS (osmotic pressure gradient). For example, FS has low salts concentration and draw solution has high salts concentration and both solutions are detached by semi-permeable membrane, so, only water particles will be extracted from FS and be moved throw the semi-permeable membrane towards the DS with high rejection rate for most

of the dissolved salts. There are various advantages for forward osmosis process such as low membrane fouling, low energy consumption compared to RO process, the ability to withstand highly contaminated feed solutions and fouling can be easily reversed using backwash with clean water. Comparing RO to FO, the driving force in RO is occurred applying pressure using a high-pressure, where pump the driving force in forward osmosis is occurred by osmotic pressure.

2.3.1 Draw solution of forward osmosis

Draw solution is defined as a solution that has high osmotic pressure. The DS osmotic pressure must be more than the FS osmotic pressure.

As noticed from equation 1 the osmotic pressure depends on different parameters such as solute concentration, molecular weight of the solute, number of ions and temperature of the solution. The solutes in the DS are the main parameter of osmotic pressure. Therefore, draw solutes with high solubility have high osmotic pressure. Several DS was observed in the previous studies and could be categorized into inorganic DS, organic DS and other types of DS such as nanoparticles DS or Polymer hydrogel particles-based DS.

2.3.1.1 Inorganic draw solution

Inorganic DSs are composed of an electrolytic solution. Though, non-electrolyte DS is possible in some cases (Achilli, Cath, & Childress, 2010). There are 14 inorganics based DS as shown in Table 3. The DS compounds were chosen out of five hundred inorganic compounds due to the osmotic pressure, low cost, and high-water solubility. Many studies have used sodium chloride (NaCl) as draw solute for FO process due to the obtainability of saline water in large quantities on the earth. Moreover, the thermodynamics of NaCl has been widely studied which makes NaCl easier to be used.

Table 3. Physical - Experimental Water Flux and Chemical Properties of Inorganic Draw Solutions (Achilli, Cath, & Childress, 2010).

Draw Solute	MW	Osmotic pressure (2.0 M)	Max solubility (g/g)	Experimental water flux (LMH)
KCl	74.60	89.30	4.6	6.337
$Ca(NO_3)_2$	164.10	108.50	7.9	5.022
NH_4Cl	53.50	87.70	7.4	5.348
$(NH_4)_2SO_4$	132.10	92.10	5.7	5.391
NH_4HCO_3	79.10	66.40	2.9	2.04
Na_2SO_4	142.00	95.20	1.8	2.14
$NaHCO_3$	84.00	46.70	1.2	2.47
NaCl	58.40	100.40	5.4	2.68
$MgSO_4$	120.40	54.80	2.8	1.54
$MgCl_2$	95.20	256.50	4.9	2.33
K_2SO_4	174.20	32.40	0.6	2.52
$KHCO_3$	100.10	79.30	2.0	2.25
KBr	119.00	89.70	4.5	2.84
$CaCl_2$	111.00	217.60	7.4	2.64

2.3.1.2 Organic draw solution

Several organic compounds have been verified as DS for FO. Glucose and fructose solutions are common DSs due to their ability to be consumed by the human body (Stache, 1989). However, the organic solution consists of non-electrolyte compounds, they tend to have high osmotic pressure because of their high solubility. Glucose was the first organic compound to be utilized as a DS in forward osmosis to supply boats with water. Moreover, glucose was tested as draw solution to concentrate tomato juice and eject water from saline water. Fructose was tested for the production of nutrients rich DS utilizing a saline FS.

Table 4. Physical - Experimental Water Flux and Chemical Properties of Organic Draw Solutions

Draw Solution	MW	Osmotic pressure (2.0 M)	Max solubility (g/g)	Experimental water flux (LMH)	References
Fructose	180.2	55.02	22.4	7.5	(Stache, 1989)
Glucose	180.2	55.02	800.0	7.5	(Stache, 1989)
Sucrose	342.3	56.81	6.1	0.35	(Stache, 1989)
Ethanol	46.1	43.93	N/A	N/A	(Stache, 1989)

2.3.1.3 Magnetic nanoparticles draw solutions

Nanoparticles are an area of comprehensive research due to the various applications in different manufactures. In water treatment, nanoparticles have been utilized as a DS in forward osmosis for desalination (M. M. Ling, Wang, & Chung, 2010). Hydrophilic magnetic nanoparticles (MNPs) have been utilized as a draw solution. The magnetic nanoparticles have been tested as DS for forward osmosis: triethyleneglycol MNPs, 2-Pyrrolidone MNPs and polyacrylic acid MNPs. Even though they are non-electrolyte, but they generate high osmotic pressure and could be recovered easily compared to organic and inorganic DSs due to their high surface area per volume ratio.

2.3.1.4 Polymer hydrogel particles-based draw solution

A new class consisting of polymer hydrogel has been utilized as draw solution in FO. Hydrogels have been defined as 3D web of polymer chain linked together utilizing physical or chemical bonds. The range of the particle size is between (50 - 150 μm). Hydrogels with ionic based particles can entice water, which increases the osmotic pressure. The polymer hydrogels have reversible volume change property in response

to pH, pressure and light. It could change from hydrophilic to hydrophobic. This characteristic makes the recovery of this draw solution much easier compared to the thermal or membrane process.

Membrane fouling is the main challenge of membrane-based osmotic processes and the major reasons for the reduction in water flux in FO are reverse solute flux (RSF) and concentration polarization (CP).

2.3.2 Concentration polarization

In general, the experimental flux is less than the theoretical flux, this is ascribed to an inescapable phenomenon identified as CP (Cath, Childress, & Elimelech, 2006; Jeffrey R. McCutcheon & Elimelech, 2006; Xiwang Zhang, Ning, Wang, & Diniz da Costa, 2014; Zhao et al., 2012). The structure of the forward osmosis membranes leads to an increase or decrease of the solution concentration at the border between the solution and membrane. Accordingly, the concentration of both solutions is different than the bulk solutions as the water is being depleted from the boundary layer (Klaysom, Hermans, Gahlaut, Van Craenenbroeck, & Vankelecom, 2013; J. R. McCutcheon, McGinnis, & Elimelech, 2005). The water flux is also decreased by the CP phenomenon (Sablani, Goosen, Al-Belushi, & Wilf, 2001). CP has been categorized into internal concentration polarization (ICP) and external concentration polarization (ECP). ECP occurs on the membrane surface. While ICP occurs within the SL. (Klaysom et al., 2013; J. R. McCutcheon et al., 2005). CP is one of the major challenges in forward osmosis membrane processes, therefore, Equation 1 has been modified in a way to consider the effect of CP in water flux as shown in Equation 2 (C. Y. Tang, She, Lay, Wang, & Fane, 2010; Xiwang Zhang et al., 2014).

$$J_w = A\sigma\Delta\pi_{EFFECTIVE} = A\sigma(\pi_{DS_A} - \pi_{FS_A}) \quad (2)$$

Where $\Delta\pi_{EFFECTIVE}$ is the effective osmotic pressure difference (net driving

force) and it is less than $\Delta\pi_b$ as a result of CP effects, $\pi_{DS_A}$is draw solution osmotic pressure at AL and $\pi_{FS_A}$is feed solution osmotic pressure at AL.

2.3.2.1 External concentration polarization (ECP)

The ECP happens on the interface between the AL and bulk FS or AL and bulk DS. In FO mode, the FSs concentration increases at FS towards AL interaction point. Therefore, Solutes build-up at AL surface which causes concentrative ECP (CECP). Thus, the gradient of osmotic pressure ($\Delta\pi$) will be decreased until it reaches the gradient of the effective osmotic pressure ($\Delta\pi_{EFFECTIVE}$), which is less than the bulk osmotic pressure gradient $\Delta\pi_b$ as shown in Figure 4. ECP appears at the AL of the membrane and can be dilutive (DECP) or concentrative based on the operation mode. In FO mode, CECP is more likely to happen. On the opposite side, DECP happens in PRO mode. As mentioned before, ECP happens due to the increase in the FS concentration on the AL. Consequently, the FS osmotic pressure increases π_{FS_A}at the AL and the net driving force decreases as shown in Equation 3. Since FO is a low energy process, the solute build-up is relatively low compared to other membrane processes, this decreases the ECP effects on water flux. The boundary layer film theory has been utilized to create a model to predict the water flux in existence of CECP in FO mode and is described as shown in Equation 3 (Jeffrey R. McCutcheon & Elimelech, 2006; McGinnis & Elimelech, 2007):

$$\frac{\pi_{FS_m}}{\pi_{FS_b}} = \exp\left(\frac{J_w}{K_F}\right) \quad (3)$$

Where π_{FS_b} and π_{FS_m} are the osmotic pressures of the feed solution in the bulk and at the membrane surface, respectively. K_F is the mass transfer coefficient on the FS of the membrane.

As the flow rate increases, turbulence could minimize the CECP influence.

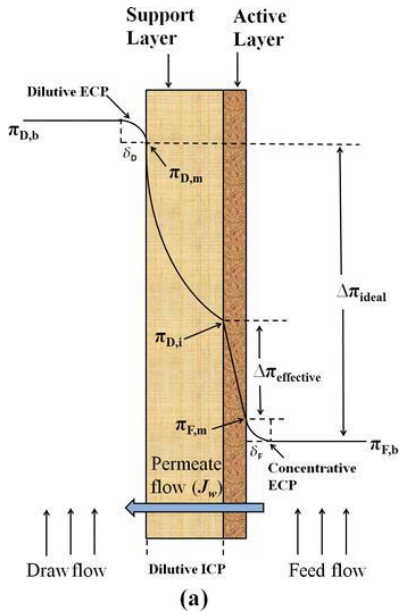

Figure 4. CECP in FO mode. (Bhinder, Shabani, & Sadrzadeh, 2018)

Dilutive external concentration polarization (DECP) is developed due to the reduction of draw solution concentration at the AL-DS interaction point which is a result of DS dilution as the water diffused from feed soution to draw solution. This reduce $\Delta\pi$ to be less than the $\Delta\pi_b$ as in the FO mode; however, the $\Delta\pi_{EFFECTIVE}$ in this mode is greater than that in FO mode that is depicted in Figure 4. The flux is calculated according to the following equation.

$$\frac{\pi_{DS_m}}{\pi_{DS_b}} = \exp\left(-\frac{J_w}{K_D}\right) \quad (4)$$

Where $\pi_{DS_m}$and π_{DS_b} are the DS osmotic pressures at the

membrane surface and bulk, and K_D is the mass transfer coefficient on the DS of the membrane. The mass transfer coefficient in both models is related to Sherwood-number which is expressed as:

$$K = \frac{Sh\ D}{d_h} \qquad (5)$$

Where D is the solute diffusion coefficient and $d_h$is the flow channel hydraulic diameter in other words the pipe diameter (Jeffrey R. McCutcheon & Elimelech, 2006).

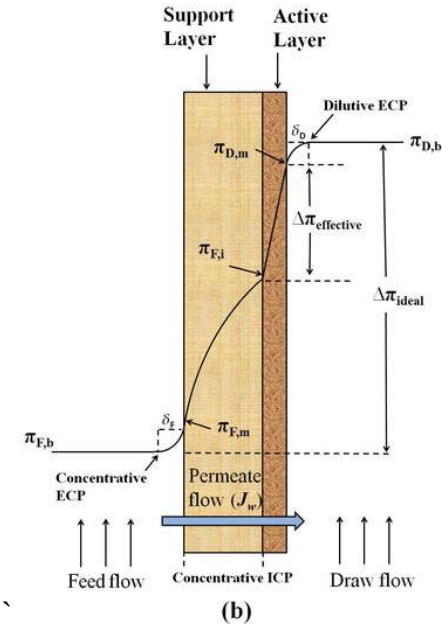

Figure 5. DECP in PRO mode. (Bhinder et al., 2018)

Generally, the ECP phenomenon in both types decreases the effective osmotic driving force in other words reduces the water flux. This unfavorable impact of the ECP can be reduced by increasing circulating flow rate or mixing that minimize the boundary layer thickness.

2.3.2.2 Internal concentration polarization

Internal concentration polarization (ICP) is developed within the SL due to asymmetrical nature of the FO membranes. Internal concentration polarization is divided into two types dilutive internal concentration polarization (DICP) which occurs in forward osmosis mode and concentrative internal concentration polarization (CICP) which occurs in PRO mode. DICP is considered as a challenging issue which negatively affects the water flux and reduces the driving force for the forward osmosis process (Cornelissen et al., 2008; Jeffrey R. McCutcheon & Elimelech, 2006; J. R. McCutcheon et al., 2005; Tan & Ng, 2008). DICP occurs in FO mode where AL is facing the FS, passage of water from the feed solution to the draw solution results in dilution of draw solution solute within the SL as in Figure 6 (b). As a result, the water flux might be reduced by 80% in some cases (Ge, Ling, & Chung, 2013). The water flux can be estimated in the presence of DICP combined with CECP in FO mode as (Jeffrey R. McCutcheon & Elimelech, 2006):

$$J_w = A\left[\pi_{DS_b}\exp(-J_w K) - \pi_{FS_b}\exp\left(\frac{J_w}{k_d}\right)\right] \quad (6)$$

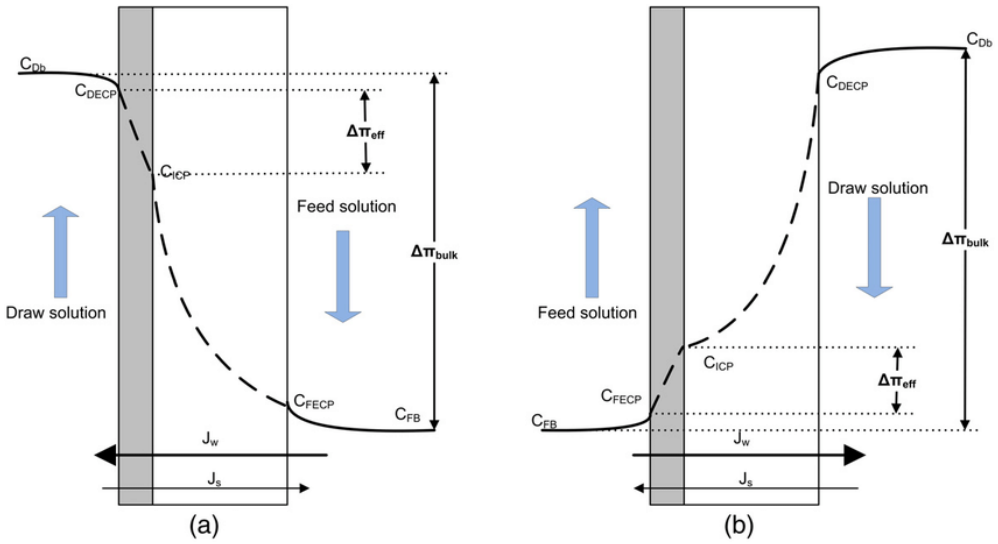

Figure 6. (a) CICP in PRO mode, (b) DICP in FO mode. (Wong, Martinez, Ramon, & Hoek, 2011)

On the other hand, while using PRO mode the concentration of the FS increased within the SL and form a polarized layer called concentrative ICP (CICP) (J. R. McCutcheon et al., 2005). The CICP phenomenon has the same concept of the CECP but different point of occurrence (J. R. McCutcheon et al., 2005). In PRO mode, the FS solutes enters the support layer due to convection phenomenon. Moreover, DS solutes diffuse through the AL due to the diffusion phenomenon into the SL. The effective driving force is reduced due to increased concentration around support layer and leads to severe flux reduction as shown in Figure 6 (a) (Cath et al., 2006; Jeffrey R. McCutcheon & Elimelech, 2006). CICP combined with DECP occurs as the membrane is operating under PRO mode. A model was developed for the PRO mode by Loeb et al. (Loeb, Van Hessen and Shahaf, 1976) and is expressed as:

$$J_w = A\left[\pi_{DS_b}\exp\left(\frac{J_w}{k_D}\right) - \pi_{FS_b}\exp(J_w K)\right] \quad (7)$$

Where K measures the easiness of solute diffusion in and out of SL and

measures the ICP severity (Xiwang Zhang et al., 2014) and it is given:

$$K = \frac{t\tau}{D\varepsilon} \quad (8)$$

Equation 6 and Equation 7 are valid for specific conditions such as low concentrations of DS using membrane parameters only and measurable experimental conditions. Hence, recent study done by Bui et al. (2015) created a model that estimates the flux considering both DECP and CICP for asymmetric and TFC membranes in PRO mode that considers hydraulic pressure gradient across the SL and is expressed as(Bui, Arena, & McCutcheon, 2015):

$$J_w = A\left[\frac{\pi_{DS_b}\exp\left(\left(\frac{-J_w}{k_D}\right)\right) - \pi_{FS_b}\exp\left(J_w\left(\frac{1}{K_F}+\frac{S}{D_F}\right)\right)}{1+\frac{B}{J_w}\left[exp\left(\frac{1}{K_F}+\frac{S}{D_F}\right) - exp\left[-\left(\frac{J_w}{k_D}\right)\right]\right]} - \Delta P\right] \quad (9)$$

A similar study was done by Bui et al, where they developed a model that estimates the water flux which accounts for both CECP and DICP for asymmetric and TFC membranes in FO mode (Bui et al., 2015). The most recent tool used to estimate the flux of asymmetric and TFC membranes is:

$$J_w = A\left[\frac{\pi_{DS_b}\exp\left(-J_w\left(\frac{1}{k_D}+\frac{S}{D_D}\right)\right) - \pi_{FS_b}\exp\left(\frac{J_w}{K_F}\right)}{1+\frac{B}{J_w}\left[exp\left(\frac{J_w}{K_F}\right) - exp\left[-J_w\left(\frac{1}{k_D}+\frac{S}{D_D}\right)\right]\right]}\right] \quad (10)$$

Where B is the membrane intrinsic solute permeability coefficient, and D_D is the solute diffusivity in the DS.

As discussed in the ICP section, the ICP is considered as a challenging issue in FO processes. In order to mitigate the ICP phenomena, the forward osmosis membranes should have a high hydrophilicity and permeability with a thin SL and a small structure

parameter (Gray, McCutcheon, & Elimelech, 2006; Jeffrey R. McCutcheon & Elimelech, 2006; Tan & Ng, 2008; C. Y. Tang et al., 2010). In addition, a draw solution with a high diffusion coefficient, Van't Hoff factor and low viscosity are required to minimize the ICP impacts (Cath et al., 2006; Gray et al., 2006; Tan & Ng, 2008). A promising way to inhibit ICP impacts is by preparing a double-skinned FO membrane with thin porous SL facing the FS that look like an ultrafiltration or nanofiltration membrane and inhibit foulants from entering into the SL and a dense AL facing the DS. This design of membrane is not commercially available yet (Tan & Ng, 2008).

2.3.3 Reverse solute flux (RSF)

Reverse solute Flux (RSF) is one of the main challenges to FO processes (Cath et al., 2006; Hancock, Maher, Latimer, Herbert, & McAuley, 2009; Zhao et al., 2012). RSF is considered as a reason for ICP in FO mode. The presence of RSF can affect the operating cost of the FO desalination processes in case of solutes permeation from DS side into the FS side owing to the additional treatment needed for the concentrated FS preceding discharge to the environment. The RSF can be reduced to an extent that can decrease the operating cost by utilizing a DS that contains multivalent ions solutes as they have lower diffusion coefficients (Cath et al., 2006; Zhao et al., 2012). However, a severe ICP occurs due to using multivalent ions that have large ions(C. Y. Tang et al., 2010; Zhao et al., 2012). In addition, the tendency of fouling can increase once being in contact with foulants in FS (Zhao, Zou, & Mulcahy, 2011). Some models have been studied to define the RSF:

$$J_s = B\Delta c \qquad (11)$$

Where J_s is the RSF, B is the membrane solute permeability coefficient, and

Δc is the difference in concentration across the semipermeable membrane.

A model was developed by Philip et al. (2010) for the purpose of RSF determination in FO process without considering the impacts of ECP on FS and DS sides (Phillip, Yong and Elimelech, 2010). Using cellulose triacetate membrane (CTA) and NaCl DS where the experimental results revealed an agreement with the model expectations (Phillip, Yong and Elimelech, 2010) And is expressed as:

$$J_s = \frac{J_w C_{DS_b}}{1 - \left(1 + \frac{J_w}{B^*}\right) \exp\left(\frac{J_w S^*}{D}\right)} \quad (12)$$

Where C_{DS_b} is DS concentration in the bulk, S^* is the membrane structural parameter, and $B^*$is the AL permeability coefficient of salt defined as:

$$B^* = \frac{D^A H}{t_A} \quad (13)$$

$$B^* = \frac{D^A H}{t_A} \quad (14)$$

Where t_s is the membrane SL thickness and t_A is the membrane AL thickness, H is the coefficient of partition, and $D^A$is the DS coefficient of diffusion in the AL.

Moreover, Suh and Lee established a model that is more accurate than Equation 12 as it highlighted all the main physical processes that happens in FO process involving the RSF, ECP, and ICP as (D. Li, Zhang, Simon, & Wang, 2013).:

$$J_s = B\left[\frac{C_{DS_b} + \left(\frac{Js}{J_w}\right)}{\exp(J_w K)\exp\left(\frac{J_w}{k_D}\right)} - \left(C_{FS_b} + \left(\frac{J_s}{J_w}\right)\right)\exp\left(\frac{J_w}{K_F}\right)\right] \quad (15)$$

A model was developed to calculate the RSF and J_s in FO mode process. The difference is that the use of B_{DS} and B_{FS} draw and feed solute permeability, respectively, instead of single solute permeability (B) as in the models as in Equation 17 and Equation 18 and both models considered the CECP and DICP:

$$J_{Ds_S} = RSF = B_{DS}\left[\frac{C_{DS_b} exp\left(-\frac{J_w S}{D}\right)}{1+\frac{B_{DS}}{J_w}\left(1-\exp\left(-\frac{J_w}{D}\right)\right)}\right] \quad (16)$$

$$J_{FS_S} = J_s = B_{FS}\left[\frac{C_{FS_b} exp\left(\frac{J_w}{K_F}\right)}{1+\frac{B_{FS}}{J_w}\left(1-\exp\left(\frac{J_w}{K_F}\right)\right)}\right] \quad (17)$$

Yong at al. used three neutral draw solutes to investigate the reverse flux: urea, , glucose and ethylene glycol (Yong, Phillip, & Elimelech, 2012). The study concluded that for rapid permeating draw solutes, ECP on the FS side of the membrane will result in additional resistance of mass transfer:

$$J_s = \frac{J_w B^*(C_{FS_b}\exp(Pe^s + Pe^\delta) - C_{DS_b})}{(B^*\exp(Pe^\delta) + J_w)\exp(Pe^s) - B^*} \quad (18)$$

Where Pe^s is the Peclet number in the SL and Pe^δ is the Peclet number in the boundary layer. In order to carry out FO, suitable membrane has to be selected.

2.4 FO membrane

2.4.1 Cellulose acetate (CA) and cellulose tri-acetate (CTA) membrane

Hydration Technologies, Inc. (HTI) developed a FO membrane that was made of Cellulose Tri-Acetate (CTA) and supported by a polyester mesh (Cath et al., 2006; Qiu, Setiawan, Wang, Tang, & Fane, 2012). This type of membranes is made by submerging rolled polymer dope into coagulants in which phase-inversion occurs and produces an asymmetric-membrane that has an AL supported by a SL (Ong & Chung, 2012; Yen, Mehnas Haja N, Su, Wang, & Chung, 2010). Preparation of the polymer dope must be using a volatile solution in the presence of added acetone to ease the evaporation process of the solution and confirm the AL formation. When CTA and Cellulose Acetate (CA) membranes are compared to other membranes such as Thin Film Composite (TFC), the fouling propensity in CA/CTA membrane was less than TFC membrane owing to its hydrophilicity nature and the strong resistance to chlorine (Ong & Chung, 2012). The water flux when CA/CTA membranes were used was observed to be below 20 LMH during FO mode with a highly concentrated DS. In addition, the RSF values were quite high compared to the RSF values when TFC membrane was used. Wang et al. (2019) tested the performance of CA membranes with MIL-53(Fe) additive in FO process (X. Wang et al., 2019). MIL-53 (Fe) was used to improve the permeability and selectivity performance of forward osmosis membranes. Utilizing DI as FS and 1.0 M NaCl as DS, the modified membrane showed higher water flux of 34.0 LMH compared to 26.8 LMH using CA commercial membrane. However, CA commercial membrane showed lower reverse solute flux (RSF) of 2.02 gMH compared to 3.12 gMH using CA/MIL-53 (Fe) membrane (X. Wang et al., 2019). Li et al. (2016) enhanced cellulose acetate membranes utilizing Polyethylene terephthalate mesh (PET) via a phase inversion process (G. Li, Wang, Hou, Bai, & Liu, 2016). The optimal FO membrane showed a water flux of 4.74 LMH and salt rejection of 96.03%

using 0.2 mol/L NaCl as the FS and 1.5 mol/L glucose as the DS in PRO mode. It was found that the PET enhanced CA membrane was able to decrease the effect of the ICP phenomenon. Ohland et al. (2019) developed a new FO membrane using hydroxyapatite particles (Hapf) functionalized by plasma treatment added to cellulose acetate substrate and a selective polyimide layer of nanocomposite membrane (Ohland, Salim, & Borges, 2019). The addition of hydroxyapatite particles (Hapf) to CA-substrate has enhanced the FO water flux from 13.8 to 18.0 LMH. This was due to lower diffusion resistance and higher hydrophilicity of the modified membrane.

2.4.2 Thin film composite (TFC) membrane

Ng et al. (2019) presented that TFC membrane properties could be affected significantly during forward osmosis process due to membrane compaction. Build-up of internal stress may be affected compaction of TFC membranes, which is related to the SL hydraulic resistance and the rate of water permeation driven by osmosis. Also, observations indicated that membranes with double-skinned might be more volatile towards osmosis-induced compaction, which may lead to a severe drop in forward osmosis performance. To achieve stabilized performance in FO process and accelerate the compaction process, FO membrane can be pre-compacted using high concentration of draw solution for a short time (Ng, Chen, Dong, & Wang, 2019). Niksefat et al. evaluated the performance of polyamide nanocomposite membrane containing silica nanoparticles created via in situ interfacial polymerizations for the forward osmosis process (Niksefat, Jahanshahi, & Rahimpour, 2014). The membrane performance was calculated utilizing 0.001M NaCl solution as feed solution and 2M NaCl solution as draw solution in two membrane orientations. The optimal TFN membrane with 0.1 wt% showed high water flux of 36 LMH compared to 18 LMH obtained using TFC membrane. In addition, TFC with 0.05 wt% silica nanoparticles gave high salt rejection

90% compared to 72% using TFC membrane. Ma et al. (2017) developed a novel TFN membrane by incorporating Zirconium (IV)-carboxylate metal-organic framework (MOF) UiO-66 nanoparticles into polyamide (PA) selective layer (Ma, Peh, Han, & Chen, 2017). TFN-U2 with 0.1 wt% showed an increase of water flux by 52% compared to TFC membrane.

2.4.3 Thin film nanocomposite (TFN) membrane

Since 2012, different studies have distributed inorganic nanomaterials in the thin polyamide AL of the TFC forward osmosis membranes to enhance the performance of their separation. M-phenylenediamine aqueous solution is reacted with trimesoyl chloride organic solution to create the polyamide layer by interfacial polymerization reaction as shown in Figure 7. Depending on the nanofillers hydrophobic/hydrophilic nature, they could be dispersed in either organic TMC or aqueous MPD phase. The typical steps of the TFN membrane fabrication process are shown in Figure 7. Nanomaterials like GO, silica, zeolites, CNTs Chitosan, and blue lemon polyoxometalate have been studied for TFN forward osmosis membranes preparation (Shakeri, Salehi, Razavi, & Mirahmadi Babaheydari, 2019; Shan et al., 2019; J. Shi et al., 2019; Zou, Smith, Lin, Martin, & He, 2019). Ma et al. developed a novel thin-film nanocomposite (TFN) membrane by incorporating Zirconiumv (IV)-carboxylate metal-organic framework (MOF) UiO-66 nanoparticles into polyamide (PA) selective layer (Ma et al., 2017). TFN-U2 with 0.1 wt% showed an increase of water flux by 52% compared to TFC membrane. Shakeri et al. investigated novel TFN forward osmosis membranes using modified super hydrophilic silica nanoparticles. Silica nano particles surface were coated utilizing super hydrophilic wheel polyoxometals. The TFN membrane containing with 0.2 wt% of nanoporticles gave water flux of 31 LMH in FO mode and RSF of 8.45 gMH. TFN with 0.2 wt% has smother surface compared to the

zero wt% of nanoparticles. However, the membranes are not appropriate for wastewaters treatment because of the surface and physicochemical properties of the rejection layer (Shakeri, Salehi, Ghorbani, Amini, & Naslhajian, 2019). Shakeri et al. (2019) enhanced the permeability and hydrophilicity properties of TFN membrane by incorporating polyoxometalate based open frameworks (POM-OFs) within the active layer of PA (Shakeri, Mighani, Salari, & Salehi, 2019). The water flux of TFN that has 500 mg/L of POM-OFs in PRO mode increased by 200% comparing it to TFC membrane.

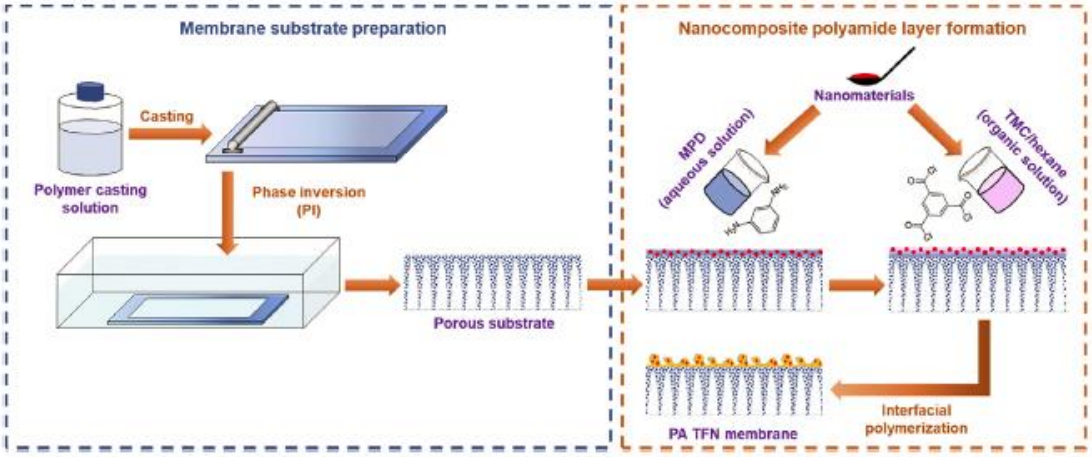

Figure 7. Interfacial polymerizaion process to fabricate TFN membrane (Akther, Phuntsho, Chen, Ghaffour, & Shon, 2019)

2.4.4 Chemically modified membranes

Newly, FO membranes have been chemically modified using different chemical modification methods to prepare new FO membranes with improved performance (Zhao et al., 2012). Arena et al. utilized a new hydrophilic polymer known as Poly-Dop-Amine (PDA) to adjust TFC RO support layer (SL) to be used in engineering

applications (Arena, McCloskey, Freeman, & McCutcheon, 2011). They showed reduction in ICP and enhancement of water. Other study done by Setiawan et al. on modified hollow fiber FO membrane with active layer (AL) that is positively charged through polyelectrolyte post treatment using Poly-Ethylene-Imine (PEI) for Poly-Amide-Imide (PAI) substrate (Setiawan, Wang, Li, & Fane, 2011). The positively charged AL allows the membrane to be used to remove heavy metals. The same group also improved a flat sheet membrane with AL that is positively charged on a substrate made of a woven fabric.

2.4.5 Other types of membranes

Shakeri et al. (2019) fabricated electro conductive membrane using graphene and polyaniline as active layer and polyamide-imide as support layer (GPANILM) (Shakeri, Salehi, & Rastgar, 2019). Also. polyaniline cross-linking (thermal treatment at 140 °C) was also applied to get higher electrical conductivity and better mechanical stability (GPANILM-140). The selectivity ratio of GPANILM membrane was 0.67 g/L in PRO mode and 0.79 g/L in FO mode. While GPANILM-140 showed lower selectivity in FO mode (0.69 g/L) and in PRO mode (0.58 g/L).

Table 5. Summary Table for Different Types of Forward Osmosis Membranes

Membrane category	**Base materials**	**Mode**	**FS**	**DS**	**Water Flux (LMH)**	**RSF (gMH)**	**Reference**
TFN	polyethersulfoe (PES)	FO PRO	DI	1 M NaCl	30.2 45.9	8.5 15.9	(Shakeri, Ghorbani, et al., 2019)

Membrane category	Base materials	Mode	FS	DS	Water Flux (LMH)	RSF (gMH)	Reference
electro-conductive nanocomposite	Support layer: polyamide-imide Active layer: dead-end filtration system	PRO PRO	DI	1 M NaCl	20.3 15.3	13.8 9.1	(Shakeri, Salehi, & Rastgar, 2019)
TFN	Support layer: PES Active layer: polyamide	PRO	DI	1 M NaCl	41.1	15.8	(Shakeri, Mighani, et al., 2019)
Hollow fiber TFC	Support layer: polymer dope Active layer: polyamide	FO	DI	1 M NaCl	30.2	3.9	(Lim, Tran, Akther, Phuntsho, & Shon, 2019)
cellulose acetate	Support layer: Polyester non-woven fabric	FO	DI	1 M NaCl	34.9	2.02	(X. Wang et al., 2019)
TFN	Support layer: Polysulfone Active layer: polyamide	PRO	10 mM of NaCl	2 M NaCl	36.5	1.5	(Niksefat et al., 2014)
TFN	Support layer: Polysulfone Active layer: polyamide	PRO	DI	1 M NaCl	36.7	7.1	(Ma et al., 2017)
Mixed matrix membrane	Cellulose acetate (CA) Chitosan	FO PRO FO	10 mM of NaCl	1 M NaCl	31.2 43.9 8	0.09 0.25 2.33	(Ghaemi & Khodakarami, 2019)

Membrane category	Base materials	Mode	FS	DS	Water Flux (LMH)	RSF (gMH)	Reference
TFN	PES	FO	DI	1 M NaCl	26.7	8.5	(Shakeri, Salehi, Razavi, et al., 2019)
		PRO			46.4	15	
	LGO-Ofs withinpolyamide	FO			18.13	6.5	
		PRO			22.9	11.3	
layer-by-layer (LbL) self-assembled	PES	FO	DI	1 M Na_2SO_4	24	1.2	(Salehi, Rastgar, & Shakeri, 2017)
		PRO			31	2.6	
	chitosan (CS) and negative graphene oxide (GO)	FO			16	2.5	
		PRO			23	3.75	
polydopamine (PDA)-modified polyethylene (DPE)-TFC	Support layer: polydopamine (PDA)-modified polyethylene (DPE)	FO	DI	1 M NaCl	53.0	14.8	(Kwon et al., 2019)
		PRO			64.8	18.1	
		FO			40.7	19.5	
TFN	PES	FO	DI	0.5 M NaCl	84.6	3.4	(Shan et al., 2019)
		PRO			114	5.17	
	GO/ OCNTs/MPD						
TFC	Active layer: modified with zwitterionic polyamide moieties	FO	DI	1 M NaCl	18.91	2.5	(Chiao et al., 2019)
					11.48	1.25	
	polysulfone supporting layer						
Nanofiber-based TFC	Support layer: chitosan	FO	DI	1.5 M NaCl	55.05	0.93	(J. Shi et al., 2019)
		PRO			64.88	2.12	

Membrane category	Base materials	Mode	FS	DS	Water Flux (LMH)	RSF (gMH)	Reference
PVDF/p-TiO2 TFC	Support layer: PVDF/p-TiO2 Active Layer: PA	FO PRO	DI	1 M NaCl	18.3 29.4	4.5 8.5	(Xuan Zhang et al., 2019)
Commercial TFC coated by Z-CNTs	Active layer: polyamide coated by Z-CNTs	FO	DI	1 M NaCl	13	3.41	(Zou, Smith, Lin, Martin, & He, 2019)
TFC with PDA/GO Interlayer	Support layer: PSf Interlayer: PDA/GO	FO	DI	1 M NaCl	24.3	3.8	(Choi, Shah, Nam, Park, & Park, 2019)
TFC-CTA	Support layer: CTA Active layer: PA	FO PRO	DI	0.5 M NaCl	9.7 12.5	13.2 20.5	(Wu, Xing, Yu, Gu, & Xu, 2018)

2.5 MXene

A CA/GO nanocomposite RO membrane developed by phase inversion technique showed efficient mechanical strength, salt rejection and hydrophilicity make

it promising membrane for seawater purification applications (Ghaseminezhad, Barikani, & Salehirad, 2019). However, rising the GO content above 1wt% shows a negative impact on the membrane in terms of fouling and therefore, this lowers the performance of the membrane (Ghaseminezhad et al., 2019). Therefore, replacing the GO with other two-dimensional material such as MXenes which have been explored as materials of membrane for water purification applications may allow a higher content of MXene in the matrix to improve the rejection and flux of the membrane. MXene has demonstrated chemical and thermal stability, mechanical flexibility, antifouling properties, excellent film forming ability, metallic electronic conductivity, hydrophilicity, etc. (Pandey et al., 2018).

One of the most, superior electrical conductivity, thermal resistance, anti-bacterial properties, high metallic conductivity availability and effortless scale up synthesis (Han, Ma, Xie, Teng, & Zhang, 2017; Rasool et al., 2017; Saththasivam, Wang, Yiming, Zhaoyang, & Mahmoud, 2019; Z. Shen et al., 2019; Si et al., 2019) Owning to these attractive properties, MXene has been extensively used in the preparation of membranes for waste water treatment, water desalination, and gas separation (Z. Shen et al., 2019). Furthermore, in polymer composites membrane applications MXene was involved to enhance the performance of the membrane.

A 40 wt.% MXene/Polyvinyl alcohol (PVA) mixed matrix composite membrane showed improved tensile strength of the membrane by three times than that of the neat PVA (Si et al., 2019). In another study, only 0.5 wt.% MXene/Polyurethane (PU) results in significant improvement of tensile strength, hardness and yield stress of PU composite membrane. Another MXene membrane showed attractive separation performance of emulsified oil/water blend and great chemical resistance to HCl, NaOH and NaCl (H. Zhang et al., 2020). Moreover, MXene membranes have been utilized for

heavy metal adsorption (Han et al., 2017). MXene membranes showed excellent antibacterial properties against *E. coli* and *B. subtilis* bacteria, makes them suitable for related-applications of anti-biofouling membrane in waste water treatment (Rasool et al., 2017), antimicrobial coatings, capacitive deionization and water refining membranes (Saththasivam, Wang, Yiming, Liu, & Mahmoud, 2019).

CHAPTER 3: EXPERIMENTAL MATERIALS AND METHODS

3.1 Materials and membrane

The membranes where fabricated by Qatar Environment and Energy Research Institute (QEERI) at Hamad Bin Khalifa University (HBKU) following the same method used in this paper (Pandey, Rasheed, Gomez, Azam, & Mahmoud, 2020). The following materials were used for the membrane fabrication. Cellulose acetate (CA) (average Mn ~30,000), Formaldehyde (CH_2O) ($\geq 34.5wt\%$), Lithium fluoride (LiF) (99.0% (F)), were purchased from Sigma-Aldrich. Commercial Whatman cellulose acetate membrane (Whatman CA, pore size 0.2 μm) was purchased from GE healthcare life science. A hydrophilic PVDF membrane (47 mm diameter) was procured from EMD Milli-pore. MXene (Ti_3AlC_2) was bought from Y-Carbon, Ltd. Acetone, PEG400 solvent, Hydrochloric acid (HCl) (35% - 38%)wt%, Sulfuric acid (H_2SO_4) (98.8%), and Acetic Acid (≥ 34.5 wt%) were procured from Merck.

3.2 Characterization

A powder X-RAY DIFRACTOMETER(XRD) were recorded using a Bruker D8 Advance (Bruker AXS, Germany) X-ray diffractometer with Cu / Ka radiation (λ= 1.5406 Å) at a current of 15.0 mA, a voltage of 40.0 kV, scanning speed of of 1°/min, step scan of 0.02 °/step. Scanning electron microscopy (SEM) was used to study the morphology of the casted membrane. This was done using FEI Quanta 650 FEG SEM, after coating the samples by gold sputter. Water contact angles for fabricated membranes were done by Rame-hart contact angle goniometers equipped with image analysis system and video camera.

3.3 Feed and draw solution for forward osmosis

Two FS were used in the forward osmosis process namely; TSE and DI. The TSE samples were brought from a sewage treatment plant located at Doha, State of

Qatar. The DS in the FO system was seawater (SW). Seawater samples were collected from corniche beach located in Doha, State of Qatar. The draw and feed solutions samples characteristics are summarized in Table 6.

Table 6. Characteristics of the Feed Solutions (i.e. DI and TSE) and the DS (i.e. Seawater).

Parameter (unit)	DI (FS)	TSE (FS)	SW (DS)	Standard Method
pH	6.9 ± 0.2	7.6 ± 0.2	7.9 ± 0.2	APHA 4500-H+ B. Electrometric Method
Temperature (°C)	25 ± 0.2	25 ± 0.2	25 ± 0.2	APHA 2550 TEMPERATURE
Turbidity (NTU)	0 ± 0.1	5.3 ± 0.1	3.1 ± 0.1	APHA 2130 B. Nephelometric Method
Conductivity (mS/cm)	0.1 ± 0.2	2.7 ± 0.2	61 ± 0.2	APHA 2510 B. Conductivity
TDS (g/L)	0.002 ± 0.005	1.7 ± 0.005	44.5 ± 0.005	APHA 2540 C. Total Dissolved Solids Dried at 180°C

3.4 Forward osmosis setup

A schematic diagram of the used FO setup is shown in Figure 8. CF042 Delrin forward osmosis membrane cell was purchased from Sterlitech. The cell dimensions are 12.7 x 8.3 x 10 cm with an inner dimension of 4.6 x 9.2 cm and a depth of 0.23 cm. The draw and feed solutions inside the cell were separated by the membrane. The feed and draw solutions were supplied by two tanks with a capacity of 10L. FS and DS were circulated through the membrane cell using two Cole-Parmer gear pumps. The flow

rate of the draw and the feed solutions were measured using two flow meters purchased from Sterlitech. A digital balance (ICS-241 Mettler Toledo) was utilized to measure the water flux in the FO system. At the beginning of the experiment, a known quantity of 6 L was used for the FS and DS. The solutions coming out from the forward osmosis cell were returned back to the same tanks. Each experiment was running for 1400 min. In addition to the synthesized membranes, a commercial forward osmosis membrane (TFC FO membrane, FTH2O (USA)) was tested.

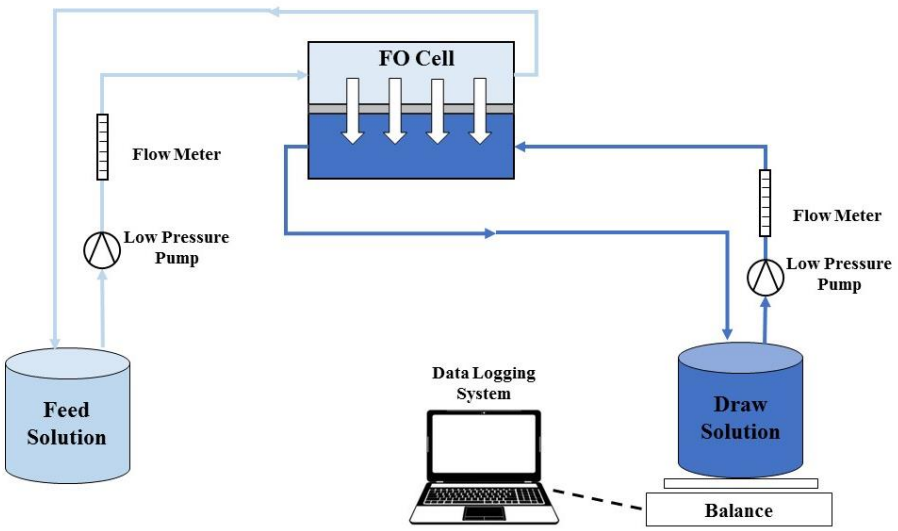

Figure 8. A schematic diagram for the bench-scale FO experimental setup.

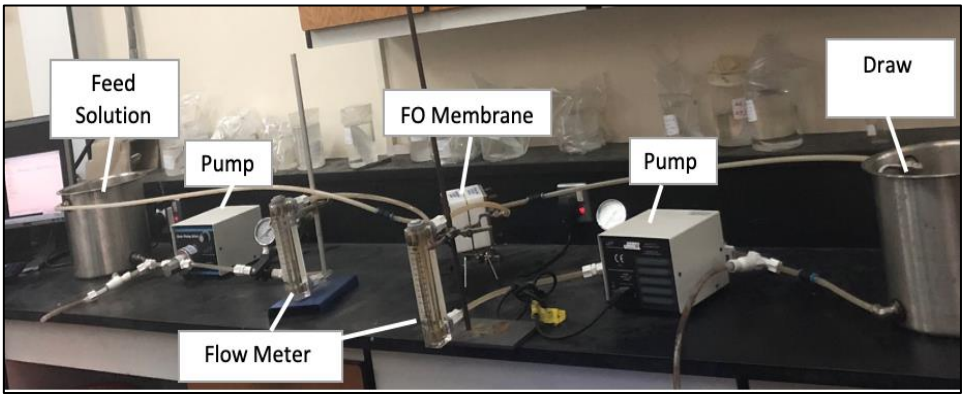

Figure 9. Forward osmosis setup.

CHAPTER 4: RESULTS & DISCUSSION

4.1 Characterization of MXene /CA membranes

Two types of cross-linked membranes were used, namely cross-linked cellulose acetate membrane (CCAM), and MXene cross-linked cellulose acetate membrane (CCAM-X%), where X% is the wt% of MXene to CA in the membrane. Five different loadings of MXene were used, namely, 0%, 2%, 4%, 6%, 8% and 10% named as CCAM-0%, CCAM-2%, CCAM-4%, CCAM-6%, CCAM8% and CCAM10%, respectively. SEM images for the surface and cross-section morphologies of CCAM-0%, CCAM-2%, CCAM-8% and CCAM-10% are described in Figure 10. MXene was found to be compatible with CA which resulted in smooth surface morphology of the membrane. CCAM-0% has less pores compared CCAM-2%, CCAM-8% and CCAM-10% (Figure 10 (a-d)). Few water channels were observed in CCAM-0% (Figure 10 (e)). However, the addition of MXene to the cross-linked CA membrane resulted in the formation of finger-like water channels (Figure 10 (f-g)). In Figure 10 (h), the finger-like water channels were not observed in CCAM-10%, because of the excessive amount of MXene in the membrane. The incorporation of MXene into CCAM enhanced the pore structure of the membrane by forming a wide homogenous finger-like water channel due to the instantaneous blending via phase inversion (J. Wang et al., 2018; Xiaojing Changa, 2014). However, the excessive amount of MXene may lead to agglomeration of particles which increase the surface roughness of the membrane (Han, Xie, & Ma, 2019). The agglomeration of the MXene blocks can be attributed to the high viscosity of the casting solution (Han et al., 2019). The addition of MXene into CCAM forms a dense hydrophilic layer which enhance the hydrophilicity of the membrane. As a result, the foulant deposition on the membrane surface is inhibited (Xiaojing Changa, 2014). The hydrophilic nature of the MXene increases the mass

transfer among the solvent and the non-solvent during the phase inversion and lead to the formation of wider pore channel (Zinadini, Zinatizadeh, Rahimi, Vatanpour, & Zangeneh, 2014).

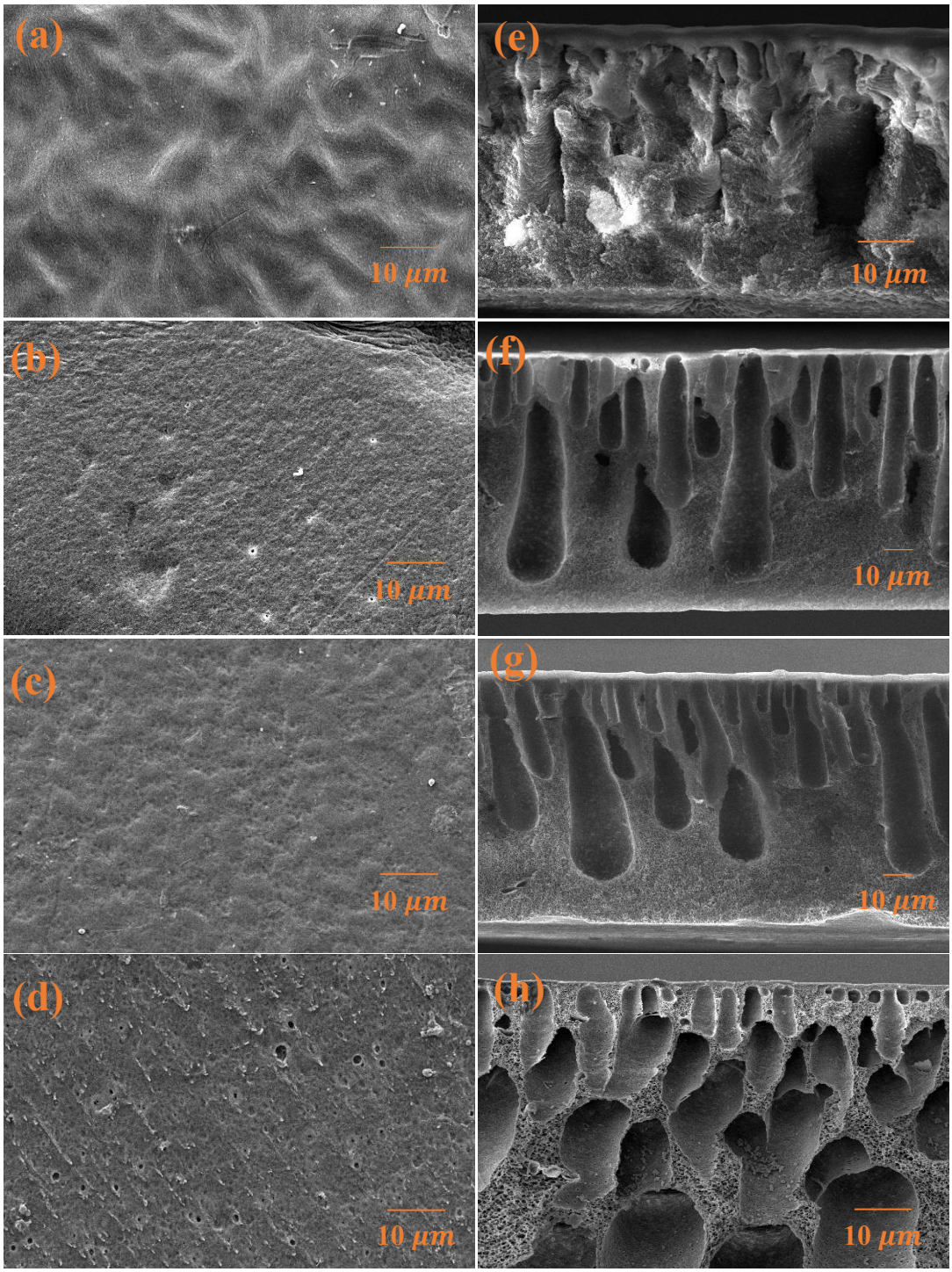

Figure 10. SEM images of prepared membranes: (a) CCAM-0% surface, (b) CCAM-2% surface, (c) CCAM-8% surface, (d) CCAM-10% surface, (e) CCAM-0% cross-section, (f) CCAM-2% cross-section, (g) CCAM-8% cross-section, and (h) CCAM-10% cross-section.

XRD was used to describe the distribution of the 2D MXene sheets in the cellulose acetate polymer matrix (Figure 11). The XRD was done at HBKU by Eng. Reem Azzam. The pristine cross-linked cellulose acetate membrane is characterized by (002) peak at ($2\theta = \sim 23°$) (Mohiuddin, Sadasivuni, Mun, & Kim, 2015). The (002) diffraction peak of the delaminated MXene is observed at ($2\theta = \sim 6.9°$). The MXene exhibited high interaction with cellulose acetate. This is due to the fact that, after adding the MXene sheets to the cellulose acetate, the (002) diffraction peak of MXene shifted by 2° to the left (R. Liu & Li, 2018). In addition, this confirms the formation of MXene-CA composite membrane and intercalation of CA chains among MXene sheets (Z. Ling et al., 2014).

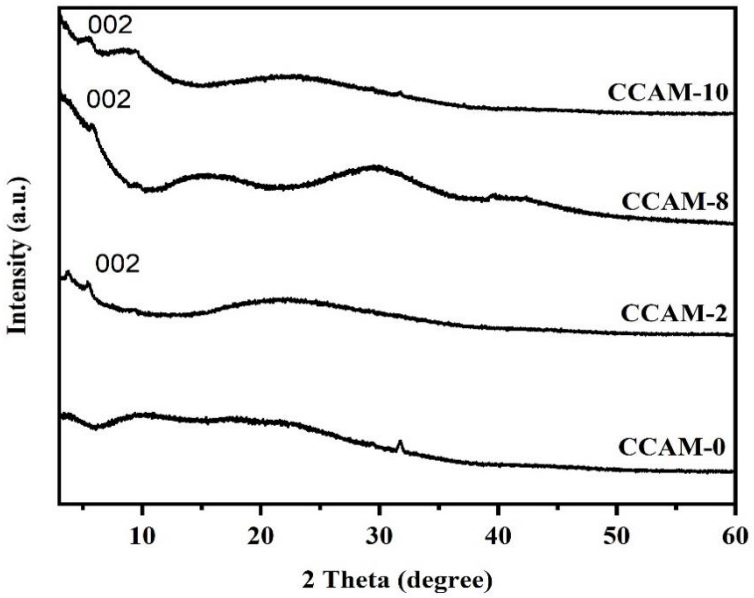

Figure 11. XRD spectra of prepared membranes CCAM-X% where X: MXene content from (0-10wt%).

The effect of MXene integration on membrane hydrophilicity was calculated by measuring the contact angle of the water (Figure 12). The measurement of contact angle was performed at HBKU by Eng. Reem Azzam. Increasing MXene from 0% to 8% improved the hydrophilicity and decreased the water contact angle by 9.3%. However, the contact angle increased by 3.5% as the MXene wt% increased from 8% to 10%, this is due to agglomerates in the casting solution and a denser functional layer (Fried, 1997).

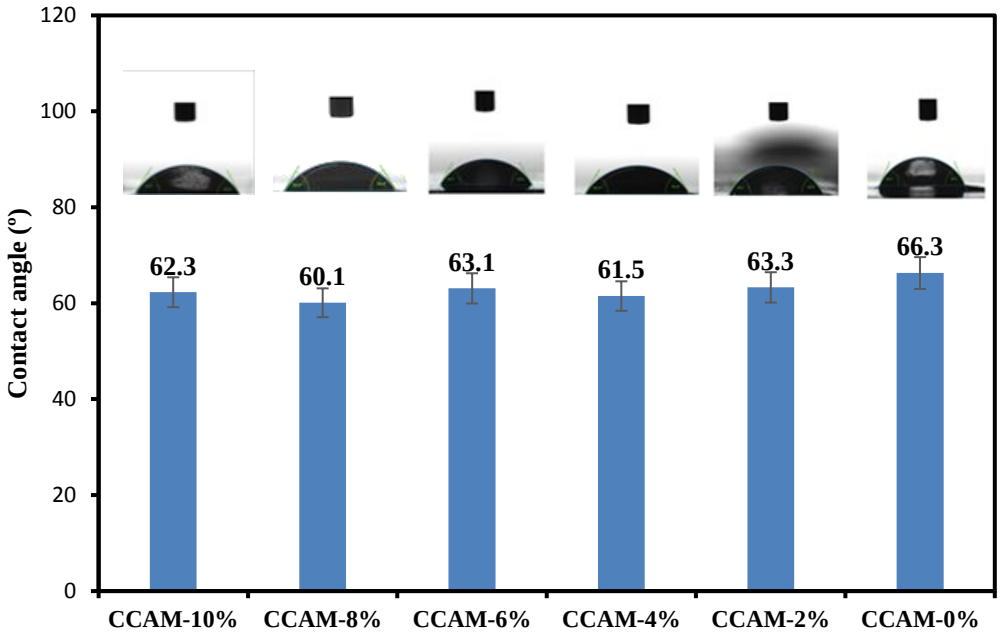

Figure 12. Water contact angle of cellulose acetate membranes loaded with different weight % of MXene.

4.2 Forward osmosis performance

4.2.1 water flux

The effect of flowrate on the membrane flux was studied using seawater as a DS and two different feed solutions. The feed solutions were DI and TSE. The flowrate of the FS and the DS was 1.2 LPM. All experiments were performed for 1400 minutes at room temperature. Figure 13 compares the membrane flux of multiple MXene wt% membranes and a TFC commercial membrane. The membrane flux (J_w) in the FO process was calculated using Equation 19:

$$J_w = \frac{\Delta V}{A_m \Delta t} \tag{19}$$

Where ΔV is the volume gradient (L), A_m is the membrane area (m^2) and t is the time interval (h).

It can be noticed from Figure 13 that water flux increased as the weight percentage of MXene increased from 0% (CCAM-0%) to 8% (CCAM-8%). The membrane flux increased by 35.5% using CCAM-8% compared to CCAM-0% using DI as the FS. While using TSE as the FS, the membrane flux increased by 28.2% using CCAM-8% compared to CCAM-0%. However, at MXene weight percentage of 10% (CCAM-10%) the membrane flux started to decrease. The membrane flux decreased by 11.1% using CCAM-10% compared to CCAM-0% using distilled water as the FS. Using TSE as the FS, the membrane flux decreased by 15.2% using CCAM-10% compared to CCAM-0%. As the MXene wt% was increased to 10%, denser functional layer and viscous casting solution are formed which will end up by membrane pores blocking and decrease the membrane flux. In addition, it can be noticed from Figure 13 that higher membrane flux was always achieved when DI was used as the FS compared to TSE as the FS. The membrane flux of the commercial TFC membrane achieved a membrane flux of 16.5 LMH and 11.2 LMH using DI and TSE as FS, respectively. CCAM-8% achieved a membrane flux of 12.2 LMH and 10.9 LMH using DI and TSE as FS, respectively. The lower membrane flux obtained when TSE was used as the FS is due to the lower osmotic pressure gradient (i.e. driving force). As shown in Table 6 the conductivity of TSE was found to be 2.1 mS/cm compared to approximately zero for DI. In addition, the lower membrane flux when using TSE as the FS could be due to the fact that TSE is rich in organic and inorganic materials which may have caused membrane fouling. Although the TFC commercial membrane showed higher membrane flux compared to CCAM-8% it should be noticed that the membrane flux of CCAM-8% decreased by only 10.7% using TSE as FS compared to DI, where the

membrane flux of the TFC commercial membrane decreased by 32.2% when using TSE as FS compared to DI. This shows that the addition of MXene to structure of the FO membrane significantly reduced the membrane fouling propensity. The enhanced antifouling feature in the modified membranes could be ascribed to the hydrophilic nature and smooth surface of the membrane (P. Liu et al., 2016; L. Shen et al., 2017). Enhanced hydrophilicity of the membrane means more strongly bounded water layer at the membrane surface which may act as a barrier for foulants and hence reduce fouling (Tiraferri, Kang, Giannelis, & Elimelech, 2012). Figure 14 shows the SEM images for a clean CCAM 8% and a TFC commercial membrane before use and an image for the same membranes after use in the FO system with TSE as the FS. The SEM images show that a foulants with a high concentration accumulated on the surface of the TFC commercial membrane (Figure 14 (b)) whereas, minimal concentration of foulants was observed on the surface of the CCAM-8% (Figure 14 (d)).

This is due to the anti-bacterial properties of the MXene that enhanced a biofouling resistance of the membrane (Rasool et al., 2017). Also, because of the hydrophilic nature of MXene that hinders the foulant accumulation on the surface of the membrane.

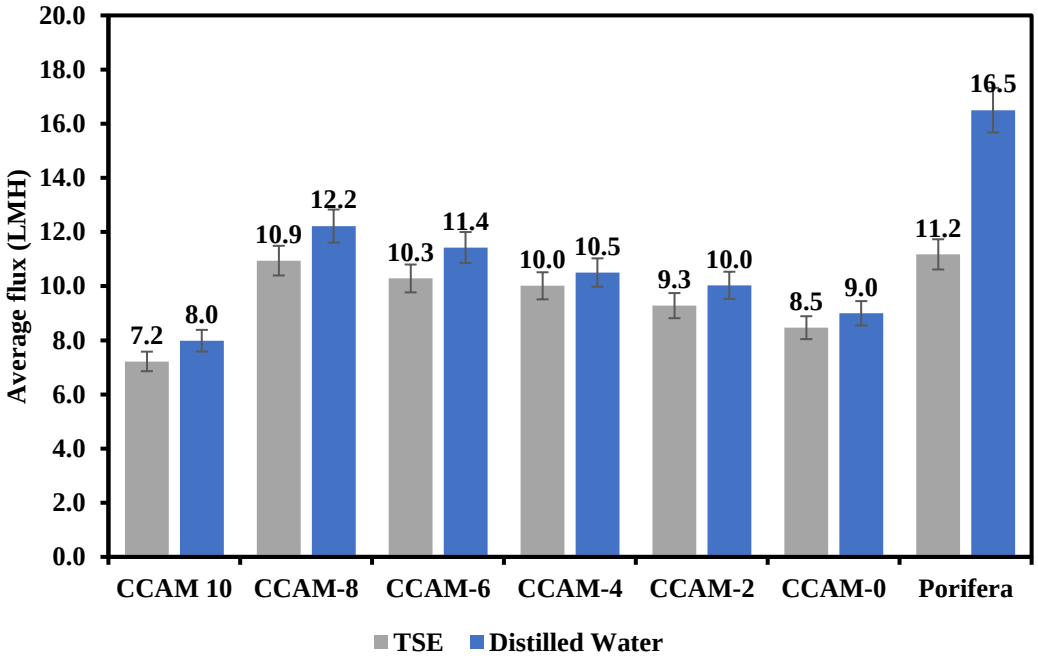

Figure 13. Membrane flux of CA/MXene ($Ti_3C_2T_x$) membrane using different MXene weight % and membrane flux of a TFC commercial membrane with DI and TSE as feed solutions.

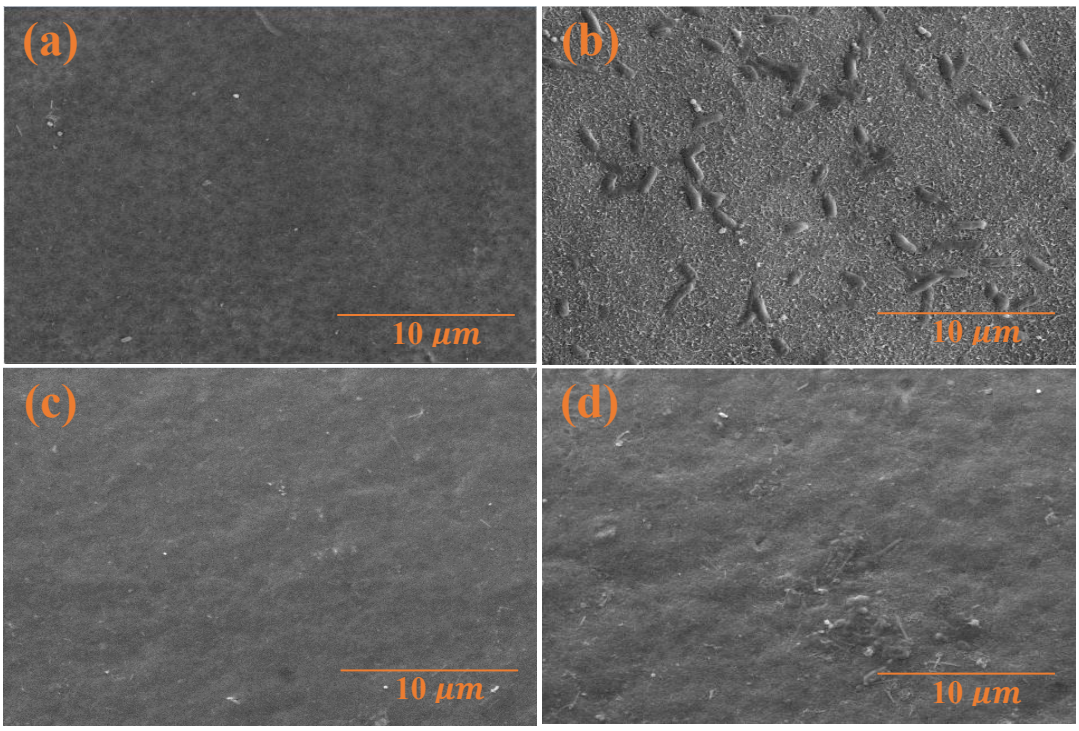

Figure 14. SEM images for a clean MXene 8% and a TFC commercial membrane before use and an images for the same membranes after use in the FO system with TSE as the FS (a) commercial clean membrane, (b) commercial membrane after use, (c) MXene 8% clean membrane, (d) MXene 8% clean membrane after use.

4.2.2 Reverse solute flux (RSF)

Reverse solute flux (RSF) is the draw solute back diffusion across the forward osmosis membrane to the FS. The reverse solute flux of the MXene and Commercial membranes were investigated, and results are presented in . The reverse solute flux (J_s) from the FO process was calculated using Equation 20:

$$J_s = \frac{C_t V_t - C_o V_o}{A_m \, \Delta t} \tag{20}$$

Where, C_o and C_t are the initial and the final salt concentration in the FS, respectively (mol/L). V_t and Vo are the final and the initial volumes of the FS, respectively (L). A and Δt are the membrane area (m^2) and the time interval (hr), respectively. As shown in , as the MXene wt% was increased the RSF increased. At CCAM-0% the RSF was 91.1 g/m^2.h and increased to 110.4 g/m^2.h at CCAM-8% when DI was used as the FS. When TSE was used as the FS the RSF increases from 72.9 g/m^2.h at CCAM-0% to 88.4 g/m^2.h at CCAM-8%. As the percentage of MXene increased to 10% the RSF decreased. Where when DI was used as the FS the RSF of CCAM-10% was 88.4 g/m^2.h and 70.5 g/m^2.h when TSE was used as the FS. The increase of the RSF with the increase of MXene weight percentage may be attributed to the pores formed between the MXene and CA matrix, which lead to increase of RSF (Shakeri, Mighani, et al., 2019). However, RSF was decreased by 26.2% using CCAM-10% compared to CCAM-0% when DI was used as the FS and 22% when TSE was used as the FS. This

can be attributed to the selective voids of the MXene membrane, where only ions with higher resistance would pass through the membrane (Shakeri, Mighani, et al., 2019). It can be also seen from Figure 15 that the RSF for the commercial membrane was much lower than the RSF for the MXene membrane. When DI was utilized as the feed solution the RSF of the commercial membrane was 34.7 g/m^2h and 17.0 g/m^2h when TSE was used as the FS. The low RSF of the commercial membrane can be attributed to its higher rejection rate.

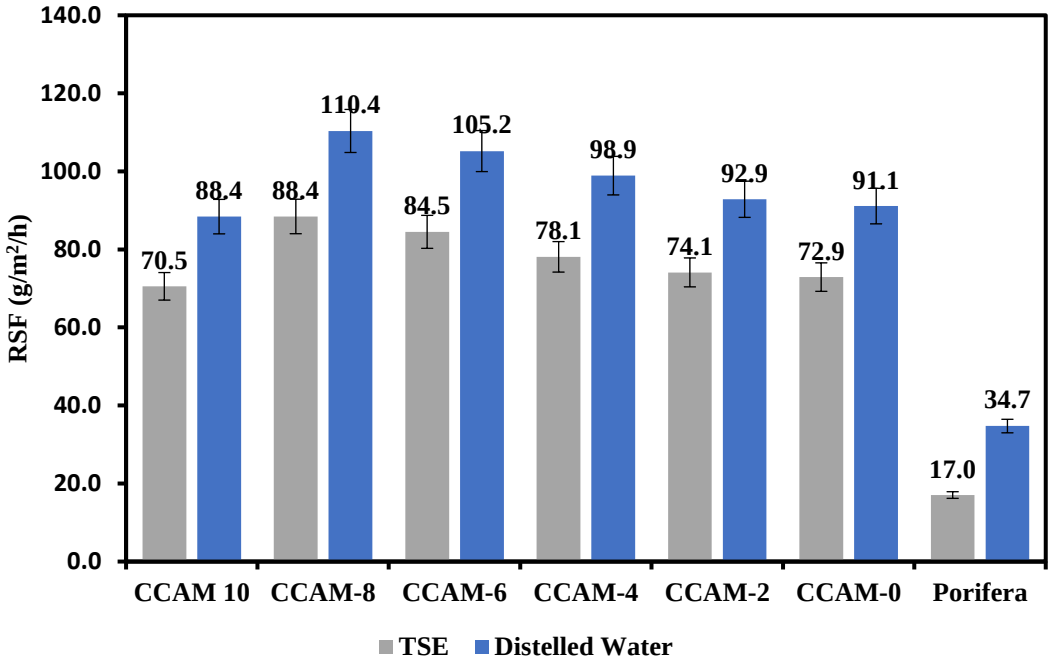

Figure 15. Reverse solute flux of CA/MXene ($Ti_3C_2T_x$) membrane using different MXene weight % and reverse solute flux of a TFC commercial membrane with DI and TSE as FS

The total dissolved solids concentration was measured in the draw solution before and after the experimental runs. As shown in Table 7 using DI as the FS, the total dissolved solids in the DS using CCAM-0%, 2%, 4%, 6%, 8%, and 10% was 45.3, 44.1, 45.2, 45.4, 45.2 and 44.8 g/L, respectively. It was observed that the DS was diluted by 15.0%, 17.5%, 18.1%, 17.6%, 19.0% and 13.8% using CCAM-0%, 2%, 4%, 6%, 8% and 10%, respectively. The corresponding dilution in TDS concentration using TSE as the FS was 13.5%, 13.3%, 17.5%, 17.0%, 16.8% and 11.0% for CCAM-0%, 2%, 4%, 6%, 8% and 10%, respectively. In the TFC commercial membrane, the dilution was 20.3% using DI as the FS and 14.7% using TSE as FS. It should be noticed that the dilution percentage in the MXene enhanced forward osmosis membrane was very comparable to the dilution percentage of the TFC commercial membrane when DI was used as the FS and when TSE was used as the FS.

Table 7. Total Dissolved Solids Concentration in the DS Before and After the FO Experiments and Dilution Percentage Using Different MXene Weight% and a TFC Commercial Membrane When DI and TSE Where Used as FS.

Membrane	Feed Solution	Initial total dissolved solids in DS (g/L)	Total dissolved solids in DS at the end of the run (g/L)	Reduction (g/L)	Reduction (%)
CCAM-0%	DI	45.3	38.5	6.8	15.0
	TSE	43.8	37.9	5.9	13.5
CCAM-2%	DI	44.1	36.4	7.72	17.5
	TSE	43.7	37.9	5.8	13.3
CCAM-4%	DI	45.2	37.0	8.2	18.1
	TSE	46.2	38.1	8.1	17.5
CCAM-6%	DI	45.4	37.4	8	17.6
	TSE	46	38.2	7.8	17.0

Membrane	Feed Solution	Initial total dissolved solids in DS (g/L)	Total dissolved solids in DS at the end of the run (g/L)	Reduction (g/L)	Reduction (%)
CCAM-8%	DI	45.2	36.6	8.6	19.0
	TSE	45.9	38.2	6.8	16.8
CCAM-10%	DI	44.8	38.6	6.2	13.8
	TSE	44.4	39.5	4.9	11.0
Commercial	DI	44.9	35.8	9.1	20.3
	TSE	44.9	38.3	6.6	14.7

CHAPTER 5: CONCLUSIONS

In this study, a new forward osmosis membrane was developed based on $Ti_3C_2T_x$ (MXene)/CA into a nanocomposite. The membrane was fabricated using the phase inversion method followed by chemical crosslinking by ($HCHO/H_2SO_4$) solution at a 50°C. The addition of MXene into the membrane substrate enhanced fouling resistance and water flux of the membrane. The membrane water contact angle decreased by 9.3 % using CCAM-8% compared to CCAM-0%. In CCAM-10%, the excessive amount of MXene have led to agglomeration of particles which increased the surface roughness of the membrane. The water flux was 9.0 LMH using CCAM-0% when distilled water was used as a feed solution. The maximum water flux was 12.2 LMH using CCAM-8%, and the minimum water flux was 8.0 LMH using CCAM-10%. Utilizing treated sewage effluent as the feed solution, the water flux was 8.5 LMH using CCAM-0%. The maximum water flux was 10.9 LMH using CCAM-8%, and the minimum water flux was 7.2 LMH using CCAM-10%. Although the TFC commercial membrane showed higher water flux compared to CCAM-8%, the resistance of the CCAM to fouling was high compared to the TFC commercial membrane. The water flux of CCAM-8% decreased by only 10.7% using TSE as FS compared to DI, where the water flux of the TFC commercial membrane decreased by 32.2% when using TSE as FS compared to DI.

REFERENCES

Achilli, A., Cath, T. Y., & Childress, A. E. (2010). Selection of inorganic-based draw solutions for forward osmosis applications. *Journal of Membrane Science, 364*(1), 233-241. doi:https://doi.org/10.1016/j.memsci.2010.08.010

Akther, N., Phuntsho, S., Chen, Y., Ghaffour, N., & Shon, H. K. (2019). Recent advances in nanomaterial-modified polyamide thin-film composite membranes for forward osmosis processes. *Journal of Membrane Science, 584*, 20-45. doi:https://doi.org/10.1016/j.memsci.2019.04.064

Altaee, A., Mabrouk, A., & Bourouni, K. (2013). A novel Forward osmosis membrane pretreatment of seawater for thermal desalination processes. *Desalination, 326*, 19-29. doi:https://doi.org/10.1016/j.desal.2013.07.008

Ang, W. L., Wahab Mohammad, A., Johnson, D., & Hilal, N. (2019). Forward osmosis research trends in desalination and wastewater treatment: A review of research trends over the past decade. *Journal of Water Process Engineering, 31*, 100886. doi:https://doi.org/10.1016/j.jwpe.2019.100886

Ardley, S., Arnold, P., Younker, J., & Rand, J. (2019). Wastewater characterization and treatment at a blueberry and carrot processing plant. *Water Resources and Industry, 21*, 100107. doi:https://doi.org/10.1016/j.wri.2019.100107

Arena, J. T., McCloskey, B., Freeman, B. D., & McCutcheon, J. R. (2011). Surface modification of thin film composite membrane support layers with polydopamine: Enabling use of reverse osmosis membranes in pressure retarded osmosis. *Journal of Membrane Science, 375*(1), 55-62. doi:https://doi.org/10.1016/j.memsci.2011.01.060

ASHGAL. (2014). Treated Sewage Effluent Networks in Qatar. In: KAHRAMAA.

Bhinder, A., Shabani, S., & Sadrzadeh, M. (2018). Effect of Internal and External

Concentration Polarizations on the Performance of Forward Osmosis Process. In.

Bromley, L. A., & Read, S. M. (1970). Multiple effect flash (MEF) evaporator. *Desalination, 7*(3), 343-391. doi:https://doi.org/10.1016/S0011-9164(00)80206-4

Brusseau, M. L., Famisan, G. B., & Artiola, J. F. (2004). 16 - CHEMICAL CONTAMINANTS. In J. F. Artiola, I. L. Pepper, & M. L. Brusseau (Eds.), *Environmental Monitoring and Characterization* (pp. 299-312). Burlington: Academic Press.

Bui, N.-N., Arena, J. T., & McCutcheon, J. R. (2015). Proper accounting of mass transfer resistances in forward osmosis: Improving the accuracy of model predictions of structural parameter. *Journal of Membrane Science, 492*, 289-302. doi:https://doi.org/10.1016/j.memsci.2015.02.001

Burn, S., Hoang, M., Zarzo, D., Olewniak, F., Campos, E., Bolto, B., & Barron, O. (2015). Desalination techniques — A review of the opportunities for desalination in agriculture. *Desalination, 364*, 2-16. doi:https://doi.org/10.1016/j.desal.2015.01.041

Cath, T. Y., Childress, A. E., & Elimelech, M. (2006). Forward osmosis: Principles, applications, and recent developments. *Journal of Membrane Science, 281*(1), 70-87. doi:https://doi.org/10.1016/j.memsci.2006.05.048

Chiao, Y.-H., Chen, S.-T., Patra, T., Hsu, C.-H., Sengupta, A., Hung, W.-S., . . . Lai, J.-Y. (2019). Zwitterionic forward osmosis membrane modified by fast second interfacial polymerization with enhanced antifouling and antimicrobial properties for produced water pretreatment. *Desalination, 469*, 114090. doi:https://doi.org/10.1016/j.desal.2019.114090

Choi, H.-g., Shah, A. A., Nam, S.-E., Park, Y.-I., & Park, H. (2019). Thin-film composite membranes comprising ultrathin hydrophilic polydopamine interlayer with graphene oxide for forward osmosis. *Desalination, 449*, 41-49. doi:https://doi.org/10.1016/j.desal.2018.10.012

Chou, S., Shi, L., Wang, R., Tang, C. Y., Qiu, C., & Fane, A. G. (2010). Characteristics and potential applications of a novel forward osmosis hollow fiber membrane. *Desalination, 261*(3), 365-372. doi:https://doi.org/10.1016/j.desal.2010.06.027

Cornelissen, E. R., Harmsen, D., de Korte, K. F., Ruiken, C. J., Qin, J.-J., Oo, H., & Wessels, L. P. (2008). Membrane fouling and process performance of forward osmosis membranes on activated sludge. *Journal of Membrane Science, 319*(1), 158-168. doi:https://doi.org/10.1016/j.memsci.2008.03.048

El-Dessouky, H., Ettouney, H., Al-Juwayhel, F., & Al-Fulaij, H. (2004). Analysis of Multistage Flash Desalination Flashing Chambers. *Chemical Engineering Research and Design, 82*(8), 967-978. doi:https://doi.org/10.1205/0263876041580668

Fiorini, P., & Sciubba, E. (2005). Thermoeconomic analysis of a MSF desalination plant. *Desalination, 182*(1), 39-51. doi:http://dx.doi.org/10.1016/j.desal.2005.03.008

Fried, J. R. (1997). Basic Principles of Membrane Technology By Marcel Mulder (University of Twente, The Netherlands). Kluwer Academic: Dordrecht. 1996. 564 pp. $255.00. ISBN 0-7823-4247-X. *Journal of the American Chemical Society, 119*(36), 8582-8582. doi:10.1021/ja975504k

Ge, Q., Ling, M., & Chung, T.-S. (2013). Draw solutions for forward osmosis processes: Developments, challenges, and prospects for the future. *Journal of Membrane Science, 442*, 225-237.

doi:https://doi.org/10.1016/j.memsci.2013.03.046

Ghaemi, N., & Khodakarami, Z. (2019). Nano-biopolymer effect on forward osmosis performance of cellulosic membrane: High water flux and low reverse salt. *Carbohydrate Polymers, 204*, 78-88. doi:https://doi.org/10.1016/j.carbpol.2018.10.005

Ghaseminezhad, S. M., Barikani, M., & Salehirad, M. (2019). Development of graphene oxide-cellulose acetate nanocomposite reverse osmosis membrane for seawater desalination. *Composites Part B: Engineering, 161*, 320-327. doi:https://doi.org/10.1016/j.compositesb.2018.10.079

Gray, G. T., McCutcheon, J. R., & Elimelech, M. (2006). Internal concentration polarization in forward osmosis: role of membrane orientation. *Desalination, 197*(1), 1-8. doi:https://doi.org/10.1016/j.desal.2006.02.003

Greenlee, L. F., Lawler, D. F., Freeman, B. D., Marrot, B., & Moulin, P. (2009). Reverse osmosis desalination: Water sources, technology, and today's challenges. *Water Research, 43*(9), 2317-2348. doi:https://doi.org/10.1016/j.watres.2009.03.010

Han, R., Ma, X., Xie, Y., Teng, D., & Zhang, S. (2017). Preparation of a new 2D MXene/PES composite membrane with excellent hydrophilicity and high flux. *RSC Advances, 7*(89), 56204-56210. doi:10.1039/C7RA10318B

Han, R., Xie, Y., & Ma, X. (2019). Crosslinked P84 copolyimide/MXene mixed matrix membrane with excellent solvent resistance and permselectivity. *Chinese Journal of Chemical Engineering, 27*(4), 877-883. doi:https://doi.org/10.1016/j.cjche.2018.10.005

Hancock, M. J., Maher, C. G., Latimer, J., Herbert, R. D., & McAuley, J. H. (2009). Can rate of recovery be predicted in patients with acute low back pain?

Development of a clinical prediction rule. *European Journal of Pain, 13*(1), 51-55. doi:https://doi.org/10.1016/j.ejpain.2008.03.007

Hanshik, C., Jeong, H., Jeong, K.-W., & Choi, S.-H. (2016). Improved productivity of the MSF (multi-stage flashing) desalination plant by increasing the TBT (top brine temperature). *Energy, 107*, 683-692. doi:https://doi.org/10.1016/j.energy.2016.04.028

Harandi, H. B., Rahnama, M., Jahanshahi Javaran, E., & Asadi, A. (2017). Performance optimization of a multi stage flash desalination unit with thermal vapor compression using genetic algorithm. *Applied Thermal Engineering, 123*, 1106-1119. doi:https://doi.org/10.1016/j.applthermaleng.2017.05.170

Hernández-Chover, V., Bellver-Domingo, Á., & Hernández-Sancho, F. (2018). Efficiency of wastewater treatment facilities: The influence of scale economies. *Journal of Environmental Management, 228*, 77-84. doi:https://doi.org/10.1016/j.jenvman.2018.09.014

Jasim, S. Y., Saththasivam, J., Loganathan, K., Ogunbiyi, O. O., & Sarp, S. (2016). Reuse of Treated Sewage Effluent (TSE) in Qatar. *Journal of Water Process Engineering, 11*, 174-182. doi:https://doi.org/10.1016/j.jwpe.2016.05.003

Klaysom, C., Hermans, S., Gahlaut, A., Van Craenenbroeck, S., & Vankelecom, I. F. J. (2013). Polyamide/Polyacrylonitrile (PA/PAN) thin film composite osmosis membranes: Film optimization, characterization and performance evaluation. *Journal of Membrane Science, 445*, 25-33. doi:https://doi.org/10.1016/j.memsci.2013.05.037

Kwon, S. J., Park, S.-H., Shin, M. G., Park, M. S., Park, K., Hong, S., . . . Lee, J.-H. (2019). Fabrication of high performance and durable forward osmosis membranes using mussel-inspired polydopamine-modified polyethylene

supports. *Journal of Membrane Science, 584*, 89-99. doi:https://doi.org/10.1016/j.memsci.2019.04.074

Li, D., Zhang, X., Simon, G. P., & Wang, H. (2013). Forward osmosis desalination using polymer hydrogels as a draw agent: Influence of draw agent, feed solution and membrane on process performance. *Water Research, 47*(1), 209-215. doi:https://doi.org/10.1016/j.watres.2012.09.049

Li, G., Wang, J., Hou, D., Bai, Y., & Liu, H. (2016). Fabrication and performance of PET mesh enhanced cellulose acetate membranes for forward osmosis. *Journal of Environmental Sciences, 45*, 7-17. doi:https://doi.org/10.1016/j.jes.2015.11.025

Li, Z.-H., Hang, Z.-Y., Lu, M., Zhang, T.-Y., & Yu, H.-Q. (2019). Difference of respiration-based approaches for quantifying heterotrophic biomass in activated sludge of biological wastewater treatment plants. *Science of The Total Environment, 664*, 45-52. doi:https://doi.org/10.1016/j.scitotenv.2019.02.007

Lim, S., Tran, V. H., Akther, N., Phuntsho, S., & Shon, H. K. (2019). Defect-free outer-selective hollow fiber thin-film composite membranes for forward osmosis applications. *Journal of Membrane Science, 586*, 281-291. doi:https://doi.org/10.1016/j.memsci.2019.05.064

Ling, M. M., Wang, K. Y., & Chung, T.-S. (2010). Highly Water-Soluble Magnetic Nanoparticles as Novel Draw Solutes in Forward Osmosis for Water Reuse. *Industrial & Engineering Chemistry Research, 49*(12), 5869-5876. doi:10.1021/ie100438x

Ling, Z., Ren, C. E., Zhao, M.-Q., Yang, J., Giammarco, J. M., Qiu, J., . . . Gogotsi, Y. (2014). Flexible and conductive MXene films and nanocomposites with high capacitance. *Proceedings of the National Academy of Sciences, 111*(47), 16676.

doi:10.1073/pnas.1414215111

Lingkungan, A. (2012). Get to know Multi Stage Flash Distillation. In.

Liu, P., Huang, T., Liu, P., Shi, S., Chen, Q., Li, L., & Shen, J. (2016). Zwitterionic modification of polyurethane membranes for enhancing the anti-fouling property. *Journal of Colloid and Interface Science, 480*, 91-101. doi:https://doi.org/10.1016/j.jcis.2016.07.005

Liu, R., & Li, W. (2018). High-Thermal-Stability and High-Thermal-Conductivity Ti3C2Tx MXene/Poly(vinyl alcohol) (PVA) Composites. *ACS Omega*, *3*(3), 2609-2617. doi:10.1021/acsomega.7b02001

Liu, Y., Ngo, H. H., Guo, W., Peng, L., Wang, D., & Ni, B. (2019). The roles of free ammonia (FA) in biological wastewater treatment processes: A review. *Environment International, 123*, 10-19. doi:https://doi.org/10.1016/j.envint.2018.11.039

Ma, D., Peh, S. B., Han, G., & Chen, S. B. (2017). Thin-Film Nanocomposite (TFN) Membranes Incorporated with Super-Hydrophilic Metal–Organic Framework (MOF) UiO-66: Toward Enhancement of Water Flux and Salt Rejection. *ACS Applied Materials & Interfaces, 9*(8), 7523-7534. doi:10.1021/acsami.6b14223

Malaeb, L., & Ayoub, G. M. (2011). Reverse osmosis technology for water treatment: State of the art review. *Desalination, 267*(1), 1-8. doi:https://doi.org/10.1016/j.desal.2010.09.001

McCutcheon, J. R., & Elimelech, M. (2006). Influence of concentrative and dilutive internal concentration polarization on flux behavior in forward osmosis. *Journal of Membrane Science, 284*(1), 237-247. doi:https://doi.org/10.1016/j.memsci.2006.07.049

McCutcheon, J. R., McGinnis, R. L., & Elimelech, M. (2005). A novel ammonia-carbon

dioxide forward (direct) osmosis desalination process. *Desalination, 174*, 1.

McGinnis, R. L., & Elimelech, M. (2007). Energy requirements of ammonia–carbon dioxide forward osmosis desalination. *Desalination, 207*(1), 370-382. doi:https://doi.org/10.1016/j.desal.2006.08.012

Mohiuddin, M., Sadasivuni, K. K., Mun, S., & Kim, J. (2015). Flexible cellulose acetate/graphene blueprints for vibrotactile actuator. *RSC Advances, 5*(43), 34432-34438. doi:10.1039/C5RA03043A

Ng, D. Y. F., Chen, Y., Dong, Z., & Wang, R. (2019). Membrane compaction in forward osmosis process. *Desalination, 468*, 114067. doi:https://doi.org/10.1016/j.desal.2019.07.007

Niksefat, N., Jahanshahi, M., & Rahimpour, A. (2014). The effect of SiO2 nanoparticles on morphology and performance of thin film composite membranes for forward osmosis application. *Desalination, 343*, 140-146. doi:https://doi.org/10.1016/j.desal.2014.03.031

Ohland, A. L., Salim, V. M. M., & Borges, C. P. (2019). Nanocomposite membranes for osmotic processes: Incorporation of functionalized hydroxyapatite in porous substrate and in selective layer. *Desalination, 463*, 23-31. doi:https://doi.org/10.1016/j.desal.2019.04.010

Ong, R. C., & Chung, T.-S. (2012). Fabrication and positron annihilation spectroscopy (PAS) characterization of cellulose triacetate membranes for forward osmosis. *Journal of Membrane Science, 394-395*, 230-240. doi:https://doi.org/10.1016/j.memsci.2011.12.046

Ong, R. C., Chung, T.-S., Helmer, B. J., & de Wit, J. S. (2012). Novel Cellulose Esters for Forward Osmosis Membranes. *Industrial & Engineering Chemistry Research, 51*(49), 16135-16145. doi:10.1021/ie302654h

. Overview on- KAHRAMAA drinking water quality requirement. (2014). Retrieved from www.km.com.qa

Pandey, R. P., Rasheed, P. A., Gomez, T., Azam, R. S., & Mahmoud, K. A. (2020). A fouling-resistant mixed-matrix nanofiltration membrane based on covalently cross-linked Ti3C2TX (MXene)/cellulose acetate. *Journal of Membrane Science, 607*, 118139. doi:https://doi.org/10.1016/j.memsci.2020.118139

Pandey, R. P., Rasool, K., Madhavan, V. E., Aïssa, B., Gogotsi, Y., & Mahmoud, K. A. (2018). Ultrahigh-flux and fouling-resistant membranes based on layered silver/MXene (Ti3C2Tx) nanosheets. *Journal of Materials Chemistry A, 6*(8), 3522-3533. doi:10.1039/C7TA10888E

. Qatar progresses with wastewater reuse plan. (2016). *Water and wastewater International*. Retrieved from http://www.waterworld.com/articles/wwi/2016/02/qatar-progresses-with-wastewater-reuse-plan.html

Qiu, C., Setiawan, L., Wang, R., Tang, C. Y., & Fane, A. G. (2012). High performance flat sheet forward osmosis membrane with an NF-like selective layer on a woven fabric embedded substrate. *Desalination, 287*, 266-270. doi:https://doi.org/10.1016/j.desal.2011.06.047

Rasool, K., Mahmoud, K., Johnson, D., I Helal, M., Berdiyorov, G., & Gogotsi, Y. (2017). Efficient Antibacterial Membrane based on Two-Dimensional Ti3C2Tx (MXene) Nanosheets. *Scientific Reports, 7*. doi:10.1038/s41598-017-01714-3

S Thabit, M., Al Hawari, A., Hafez Ammar, M., Zaidi, J., Zaragoza, G., & Altaee, A. (2019). *Evaluation of forward osmosis as a pretreatment process for multi stage flash seawater desalination* (Vol. 461).

Sablani, S. S., Goosen, M. F. A., Al-Belushi, R., & Wilf, M. (2001). Concentration

polarization in ultrafiltration and reverse osmosis: a critical review. *Desalination, 141*(3), 269-289. doi:https://doi.org/10.1016/S0011-9164(01)85005-0

Salehi, H., Rastgar, M., & Shakeri, A. (2017). Anti-fouling and high water permeable forward osmosis membrane fabricated via layer by layer assembly of chitosan/graphene oxide. *Applied Surface Science, 413*, 99-108. doi:https://doi.org/10.1016/j.apsusc.2017.03.271

Salgot, M., & Folch, M. (2018). Wastewater treatment and water reuse. *Current Opinion in Environmental Science & Health, 2*, 64-74. doi:https://doi.org/10.1016/j.coesh.2018.03.005

Saththasivam, J., Wang, K., Yiming, W., Liu, Z., & Mahmoud, K. A. (2019). A flexible Ti3C2Tx (MXene)/paper membrane for efficient oil/water separation. *RSC Advances, 9*(29), 16296-16304. doi:10.1039/C9RA02129A

Saththasivam, J., Wang, K., Yiming, W., Zhaoyang, L., & Mahmoud, K. (2019). A flexible Ti 3 C 2 T x (MXene)/paper membrane for efficient oil/water separation. *RSC Advances, 9*, 16296-16304. doi:10.1039/C9RA02129A

Setiawan, L., Wang, R., Li, K., & Fane, A. G. (2011). Fabrication of novel poly(amide–imide) forward osmosis hollow fiber membranes with a positively charged nanofiltration-like selective layer. *Journal of Membrane Science, 369*(1), 196-205. doi:https://doi.org/10.1016/j.memsci.2010.11.067

Shaffer, D. L., Werber, J. R., Jaramillo, H., Lin, S., & Elimelech, M. (2015). Forward osmosis: Where are we now? *Desalination, 356*, 271-284. doi:https://doi.org/10.1016/j.desal.2014.10.031

Shakeri, A., Mighani, H., Salari, N., & Salehi, H. (2019). Surface modification of forward osmosis membrane using polyoxometalate based open frameworks for

hydrophilicity and water flux improvement. *Journal of Water Process Engineering, 29*, 100762. doi:https://doi.org/10.1016/j.jwpe.2019.02.002

Shakeri, A., Salehi, H., Ghorbani, F., Amini, M., & Naslhajian, H. (2019). Polyoxometalate based thin film nanocomposite forward osmosis membrane: Superhydrophilic, anti-fouling, and high water permeable. *Journal of Colloid and Interface Science, 536*, 328-338. doi:https://doi.org/10.1016/j.jcis.2018.10.069

Shakeri, A., Salehi, H., & Rastgar, M. (2019). Antifouling electrically conductive membrane for forward osmosis prepared by polyaniline/graphene nanocomposite. *Journal of Water Process Engineering, 32*, 100932. doi:https://doi.org/10.1016/j.jwpe.2019.100932

Shakeri, A., Salehi, H., Razavi, S. R., & Mirahmadi Babaheydari, S. M. (2019). Blue lemon@quaternary graphene oxide open frameworks: As a novel nanostructure for performance enhancement of thin film nanocomposite forward osmosis membrane. *Chemical Engineering Research and Design, 148*, 451-459. doi:https://doi.org/10.1016/j.cherd.2019.06.035

Shan, M., Kang, H., Xu, Z., Li, N., Jing, M., Hu, Y., . . . Liu, L. (2019). Decreased cross-linking in interfacial polymerization and heteromorphic support between nanoparticles: Towards high-water and low-solute flux of hybrid forward osmosis membrane. *Journal of Colloid and Interface Science, 548*, 170-183. doi:https://doi.org/10.1016/j.jcis.2019.04.014

Sharma, A., Syed, Z., Brighu, U., Gupta, A. B., & Ram, C. (2019). Adsorption of textile wastewater on alkali-activated sand. *Journal of Cleaner Production, 220*, 23-32. doi:https://doi.org/10.1016/j.jclepro.2019.01.236

Shen, L., Wang, X., Li, R., Yu, H., Hong, H., Lin, H., . . . Liao, B.-Q. (2017).

Physicochemical correlations between membrane surface hydrophilicity and adhesive fouling in membrane bioreactors. *Journal of Colloid and Interface Science, 505*, 900-909. doi:https://doi.org/10.1016/j.jcis.2017.06.090

Shen, Z., Chen, W., Xu, H., Yang, W., Kong, Q., Wang, A., . . . Shang, J. (2019). Fabrication of a Novel Antifouling Polysulfone Membrane with in Situ Embedment of Mxene Nanosheets. *International Journal of Environmental Research and Public Health, 16*, 4659. doi:10.3390/ijerph16234659

Shi, J., Kang, H., Li, N., Teng, K., Sun, W., Xu, Z., . . . Liu, Q. (2019). Chitosan sub-layer binding and bridging for nanofiber-based composite forward osmosis membrane. *Applied Surface Science, 478*, 38-48. doi:https://doi.org/10.1016/j.apsusc.2019.01.148

Shi, L., Chou, S. R., Wang, R., Fang, W. X., Tang, C. Y., & Fane, A. G. (2011). Effect of substrate structure on the performance of thin-film composite forward osmosis hollow fiber membranes. *Journal of Membrane Science, 382*(1), 116-123. doi:https://doi.org/10.1016/j.memsci.2011.07.045

Si, J.-Y., Tawiah, B., Sun, W.-L., Lin, B., Wang, C., Yuen, A. C. Y., . . . Yeoh, G. (2019). Functionalization of MXene Nanosheets for Polystyrene towards High Thermal Stability and Flame Retardant Properties. *Polymers, 11*, 976. doi:10.3390/polym11060976

Stache, K. (1989).

Tan, C. H., & Ng, H. Y. (2008). Modified models to predict flux behavior in forward osmosis in consideration of external and internal concentration polarizations. *Journal of Membrane Science, 324*(1), 209-219. doi:https://doi.org/10.1016/j.memsci.2008.07.020

Tang, C. Y., She, Q., Lay, W. C. L., Wang, R., & Fane, A. G. (2010). Coupled effects

of internal concentration polarization and fouling on flux behavior of forward osmosis membranes during humic acid filtration. *Journal of Membrane Science, 354*(1), 123-133. doi:https://doi.org/10.1016/j.memsci.2010.02.059

Tang, J., Zhang, C., Shi, X., Sun, J., & Cunningham, J. A. (2019). Municipal wastewater treatment plants coupled with electrochemical, biological and bio-electrochemical technologies: Opportunities and challenge toward energy self-sufficiency. *Journal of Environmental Management, 234*, 396-403. doi:https://doi.org/10.1016/j.jenvman.2018.12.097

Tiraferri, A., Kang, Y., Giannelis, E. P., & Elimelech, M. (2012). Superhydrophilic Thin-Film Composite Forward Osmosis Membranes for Organic Fouling Control: Fouling Behavior and Antifouling Mechanisms. *Environmental Science & Technology*, *46*(20), 11135-11144. doi:10.1021/es3028617

Ullah, I., Rasul, M., & Khan, M. M. (2013). *An overview of solar thermal desalination technologies*.

Wang, J., Chen, P., Shi, B., Guo, W., Jaroniec, M., & Qiao, S.-Z. (2018). A Regularly Channeled Lamellar Membrane for Unparalleled Water and Organics Permeation. *Angewandte Chemie International Edition, 57*(23), 6814-6818. doi:10.1002/anie.201801094

Wang, K. Y., Chung, T.-S., & Amy, G. (2012). Developing thin-film-composite forward osmosis membranes on the PES/SPSf substrate through interfacial polymerization. *AIChE Journal, 58*(3), 770-781. doi:10.1002/aic.12635

Wang, K. Y., Yang, Q., Chung, T.-S., & Rajagopalan, R. (2009). Enhanced forward osmosis from chemically modified polybenzimidazole (PBI) nanofiltration hollow fiber membranes with a thin wall. *Chemical Engineering Science, 64*(7), 1577-1584. doi:https://doi.org/10.1016/j.ces.2008.12.032

Wang, X., Ba, X., Cui, N., Ma, Z., Wang, L., Wang, Z., & Gao, X. (2019). Preparation, characterisation, and desalination performance study of cellulose acetate membranes with MIL-53(Fe) additive. *Journal of Membrane Science, 590*, 117057. doi:https://doi.org/10.1016/j.memsci.2019.04.061

WATER STATISTICS In The State of Qatar, 2015. (2017). Retrieved from http://www.mdps.gov.qa/en/knowledge/ReportsandStudies/WaterStats2016En.pdf

Wong, M., Martinez, K., Ramon, G., & Hoek, E. (2011). Impacts of operating conditions and solution chemistry on osmotic membrane structure and performance. *Desalination, 287*. doi:10.1016/j.desal.2011.10.013

Wu, Q.-Y., Xing, X.-Y., Yu, Y., Gu, L., & Xu, Z.-K. (2018). Novel thin film composite membranes supported by cellulose triacetate porous substrates for high-performance forward osmosis. *Polymer, 153*, 150-160. doi:https://doi.org/10.1016/j.polymer.2018.08.017

Xiaojing Changa, b., 1, Zhenxing Wanga,1, Shuai Quana,1, Yanchao Xua,1, Zaixing Jianga,1, Lu Shaoa,∗,1. (2014). Exploring the synergetic effects of graphene oxide (GO) and polyvinylpyrrodione (PVP) on poly(vinylylidenefluoride) (PVDF) ultrafiltration membrane performance. *Applied Surface Science*.

Yen, S. K., Mehnas Haja N, F., Su, M., Wang, K. Y., & Chung, T.-S. (2010). Study of draw solutes using 2-methylimidazole-based compounds in forward osmosis. *Journal of Membrane Science, 364*(1), 242-252. doi:https://doi.org/10.1016/j.memsci.2010.08.021

Yong, J. S., Phillip, W. A., & Elimelech, M. (2012). Coupled reverse draw solute permeation and water flux in forward osmosis with neutral draw solutes. *Journal of Membrane Science, 392-393*, 9-17.

doi:https://doi.org/10.1016/j.memsci.2011.11.020

Zhang, H., Wang, Z., Shen, Y., Mu, P., Wang, Q., & Li, J. (2020). Ultrathin 2D Ti3C2Tx MXene membrane for effective separation of oil-in-water emulsions in acidic, alkaline, and salty environment. *Journal of Colloid and Interface Science, 561*, 861-869. doi:https://doi.org/10.1016/j.jcis.2019.11.069

Zhang, X., Ning, Z., Wang, D. K., & Diniz da Costa, J. C. (2014). Processing municipal wastewaters by forward osmosis using CTA membrane. *Journal of Membrane Science, 468*, 269-275. doi:https://doi.org/10.1016/j.memsci.2014.06.016

Zhang, X., Xiong, S., Liu, C.-X., Shen, L., Ding, C., Guan, C.-Y., & Wang, Y. (2019). Confining migration of amine monomer during interfacial polymerization for constructing thin-film composite forward osmosis membrane with low fouling propensity. *Chemical Engineering Science, 207*, 54-68. doi:https://doi.org/10.1016/j.ces.2019.06.010

Zhao, S., Zou, L., & Mulcahy, D. (2011). Effects of membrane orientation on process performance in forward osmosis applications. *Journal of Membrane Science, 382*(1), 308-315. doi:https://doi.org/10.1016/j.memsci.2011.08.020

Zhao, S., Zou, L., Tang, C. Y., & Mulcahy, D. (2012). Recent developments in forward osmosis: Opportunities and challenges. *Journal of Membrane Science, 396*, 1-21. doi:https://doi.org/10.1016/j.memsci.2011.12.023

Zinadini, S., Zinatizadeh, A. A., Rahimi, M., Vatanpour, V., & Zangeneh, H. (2014). Preparation of a novel antifouling mixed matrix PES membrane by embedding graphene oxide nanoplates. *Journal of Membrane Science, 453*, 292-301. doi:https://doi.org/10.1016/j.memsci.2013.10.070

Zou, S., Smith, E. D., Lin, S., Martin, S. M., & He, Z. (2019). Mitigation of bidirectional solute flux in forward osmosis via membrane surface coating of zwitterion

functionalized carbon nanotubes. *Environment International, 131*, 104970. doi:https://doi.org/10.1016/j.envint.2019.104970